

AN ABSTRACT OF THE THESIS OF

Justin J. Provolt for the degree of Master of Science in Environmental Engineering presented on June 6, 2013.

Title: Evaluation of Apatite II™ for Removal of Copper and Zinc from Highway Stormwater Runoff: Laboratory and Field Experiments

Abstract approved: _____

Jeffrey A. Nason

Current best management practices (BMPs) for stormwater treatment are not able to adequately remove heavy metals to levels which do not adversely affect aquatic life. Copper is commonly found in highway stormwater runoff, with the primary source being brake pad wear. Copper is of particular concern due to inhibitory effects on juvenile salmon at low concentrations. In the current study, Apatite II™, a biogenic fish-bone based adsorbent, was evaluated for copper and zinc removal from stormwater. Batch, column, and field experiments were performed to examine the potential of Apatite II™ to remove copper from stormwater. In both batch and continuous systems, the release of phosphate and calcium were observed and Apatite II™ achieved high removal efficiencies. In column experiments, copper breakthrough was independent of influent concentration. The extent of copper removal with Apatite II™ appears to be controlled by the solubility of copper containing precipitates and is a strong function of pH. Precipitation of insoluble metal oxides/hydroxides/phosphates was the primary mechanism of copper removal; the release of phosphate due to dissolution of the Apatite II™ buffered the pH and induced precipitation of copper and zinc. A field site along Highway 22 in Salem, OR was identified for field experiments. Preliminary sampling at the site indicated sufficient flow and dissolved copper to implement a field-scale Apatite

IITM filter. Engineering concepts were used to design, construct, and install a field-scale filter aimed at removing copper from actual highway stormwater runoff. Apatite IITM shows potential as a low-cost alternative to effectively remove copper and zinc to trace levels in highway stormwater runoff.

©Copyright by Justin J. Provolt

June 6, 2013

All Rights Reserved

Evaluation of Apatite II™ for Removal of Copper and Zinc from Highway Stormwater
Runoff: Laboratory and Field Experiments

by
Justin J. Provolt

A THESIS
submitted to
Oregon State University

in partial fulfillment of
the requirements for the
degree of
Master of Science

Presented June 6, 2013
Commencement June 2013

Master of Science thesis of Justin J. Provolt presented on June 6, 2013.

APPROVED:

Major Professor, representing Environmental Engineering

Head of the School of Chemical, Biological, and Environmental Engineering

Dean of the Graduate School

I understand that my thesis will become part of the permanent collection of Oregon State University libraries. My signature below authorizes release of my thesis to any reader upon request.

Justin J. Provolt, Author

ACKNOWLEDGEMENTS

I have many individuals to thank who helped in the completion of this thesis. Some of these people include the staff of the Chemical, Biological, and Environmental Engineering department, Kathryn Motter of the IWW Collaboratory, Dr. Mohammed Azizian, Manfred Dittrich, Cameron Oden and friends and family who have supported me through my education. A special thanks to my advisor Dr. Jeffrey Nason for the opportunity and Oregon Department of Transportation for funding that opportunity. Research was highly enjoyable due to Brian Rowbotham's entertainment in the laboratory and Brian Smith's commendable hole digging skills.

TABLE OF CONTENTS

	<u>Page</u>
1 Introduction	1
1.1 Objectives	2
1.2 Approach.....	3
2 Literature Review	4
2.1 Copper in highway stormwater runoff.....	4
2.2 Previous laboratory experiments with Apatite II™	5
2.3 Filtration based BMPs for metals removal	8
2.4 Removal of metals with compost.....	11
3 Materials and Methods	15
3.1 Apatite II™	15
3.2 Reagents.....	15
3.3 Laboratory Experiments.....	16
3.3.1 Batch Studies	16
3.3.1 Column Studies.....	18
3.4 Stormwater Sampling.....	19
3.4.1 Site Description	19
3.4.2 Sampling Equipment	20
3.4.3 Field Sampling Procedure.....	22
3.5 Laboratory Methods.....	23
3.5.1 Sample Fractionation	23

TABLE OF CONTENTS (Continued)		<u>Page</u>
3.5.2	Total Suspended Solids (TSS)	25
3.5.3	pH and Conductivity	25
3.5.4	Cations	25
3.5.4	Anions	25
3.5.5	Dissolved Organic Carbon (DOC).....	26
3.5.6	Cleaning Procedure.....	26
4	Laboratory Results	28
4.1	Equilibrium Batch Studies	28
4.2	Column Studies	32
4.2.1	Estimation of bed life at full-scale.....	39
5	Field Site Design and Construction	42
5.1	Site Selection	42
5.2	Estimating Stormwater Runoff	43
5.3	Stormwater Sampling.....	46
5.4	Site Survey and Permitting	50
5.5	Filter bed layout	52
5.6	Inlet Structure.....	55
5.6	Outlet Structure	57
5.7	Filter bed construction	60
5.8	Installation of filter	64
6	Conclusions	72
6.1	Results from laboratory experiments	72

TABLE OF CONTENTS (Continued)		<u>Page</u>
6.1.1 Practical Implications from laboratory experiments.....		73
6.2 Results from field experiments		74
6.2.1 Practical Implications from field experiments.....		74
6.3 Future work		75
Appendix		77
Hydraulic Conductivity Experiments		77
Compost Batch Equilibrium Experiment.....		79
Calculation of bed life for hypothetical full-scale system		80

LIST OF FIGURES

<u>Figure</u>	<u>Page</u>
Figure 1. Apatite II™ as received from PIMS NW, Inc.	15
Figure 2. Batch experiment process diagram.....	17
Figure 3. Packed bed column flow diagram	19
Figure 4. Mission Street Aerial View	20
Figure 5. Highway 22 sampling installation.....	21
Figure 6. Calibration curve for combination Thel-mar weir.....	22
Figure 7. Sample Processing Flow Diagram.....	24
Figure 8. Copper and zinc removal in single-element batch studies (final pH 7.0-7.7) ...	29
Figure 9. Single-element batch studies with the addition of NOM (final pH 6.6-7.0).....	31
Figure 10. Sieved Apatite II™ media before (left) and after column experiment (right). 34	
Figure 11. Breakthrough of copper and zinc in column experiments.....	35
Figure 12. Relative Breakthrough (C/C_0) of copper and zinc in column experiments	35
Figure 13. Effluent phosphate during column experiments.....	36
Figure 14. Effluent calcium during column experiments	36
Figure 15. Effluent pH during column experiments	37
Figure 16. Hypothetical design incorporating Apatite II™ into a media filter drain	40
Figure 17. Existing ground at Highway 22 site (Salem, OR).....	43

LIST OF FIGURES (Continued)

Page

Figure 18. Estimated flowrate and accumulated volume during December 2010.....	44
Figure 19. Hypothetical volume to breakthrough for 4' x 4' filter bed, hydraulic loading rate (HLR), and volume treated (full flow) during December 2010.....	46
Figure 20. Estimate of flowrate and accumulated volume for storm event on 3/5/2013..	47
Figure 21. Flow and sampling events recorded by ISCO 6712 on 3/5/2013.....	48
Figure 22. Water quality data from six analyzed stormwater samples on 3/5/2013.....	49
Figure 23. Overview of field site	51
Figure 24. Cross section of site along existing 12" HDPE pipe	52
Figure 25. Layout of filter bed configuration	53
Figure 26. Schematic of inlet structure (dimensions are in feet)	56
Figure 27. Constructed inlet box.....	57
Figure 28. Schematic of outlet box (dimensions are in feet)	58
Figure 29. Comparison of v-notch weir angles.....	59
Figure 30. Constructed outlet box.....	60
Figure 31. Filter bed frame and floor.....	61
Figure 32. Constructed filter bed	62
Figure 33. 2" PVC under drain and 1 ½" PVC delivery system.....	63
Figure 34. Constructed filter lid.....	64
Figure 35. Installed security fence	65

LIST OF FIGURES (Continued)

Page

Figure 36. Installed inlet structure	66
Figure 37. Installed filter bed with polyethylene sheeting.....	67
Figure 38. Installed outlet structure	68
Figure 39. Geotextile material installed between gravel and Apatite II™ layers.....	69
Figure 40. Installed 4” layer of Apatite II™ media	70
Figure 41. Final gravel layer installed in filter bed.....	71
Figure 42. Layout and thickness of material layers	77
Figure 43. Hydraulic conductivity values (slope) fitted from experimental data	78

LIST OF TABLES

<u>Table</u>	<u>Page</u>
Table 1. Combination v-notch/rectangular weir equation	22
Table 2. Average pH, phosphate, and calcium at equilibrium in batch studies	30
Table 3. Average pH, phosphate, and calcium at equilibrium in batch studies with NOM	32
Table 4. Comparison of removal capacities calculated from the column and batch experiments	38
Table 5. Field site selection characteristics.....	42
Table 6. Summary of headloss calculations.....	54
Table 7. Comparison of total system flow and flow through the bed.....	56
Table 8. Average equilibrium concentrations of dissolved copper in batch studies.....	80
Table 9. Average anion concentrations (mg/L) at equilibrium in batch studies.....	80

Evaluation of Apatite II™ for Removal of Copper and Zinc from Highway Stormwater Runoff: Laboratory and Field Experiments

1 Introduction

Heavy metal contamination of surface waters is of major concern due to the resulting toxic effects on aquatic life. The discharge of stormwater into surface water represents a significant source of metals such as Cu, Cd, Zn, Pb, Ni and Cr (Kayhanian 2010, Howell 1979, Hewitt and Rashed 1988, Makepeace, Smith and Stanley 1995). This study is primarily concerned with copper due to its inhibitory effects on juvenile salmon at low concentrations. Recent studies have found that juvenile Coho salmon exposed to 2 µg/L of dissolved copper for 3 hours had inhibited predator avoidance behavior and olfactory function (Sandahl et al. 2007). Anthropogenic sources that contribute to copper in highway stormwater runoff include brake pad wear, residual engine oil, and atmospheric deposition. The most significant source of copper in highway stormwater runoff is brake pad wear (Davis, Shokouhian and Ni 2001). Current regulation stipulated by Oregon Department of Environmental Quality require that the concentration of total copper be below 20 µg/L in industrial stormwater (ODEQ 2012). Additionally, under section 7 of the Endangered Species Act (ESA), the National Marine Fisheries Service (NMFS) must issue biological opinions on transportation projects likely to adversely affect threatened and endangered aquatic species. These assessments can result in cost inducing project delays and additional stormwater treatment systems may be required for current and future transportation projects.

Current technologies such as filter strips and retention ponds are able to effectively remove both particulate and dissolved forms of copper and zinc, but typically do a better job of removing particulate metals (Wright Water Engineers and Geosyntec Consultants 2011). At best, current stormwater best management practices (BMPs) are only able to remove dissolved copper to approximately 5 µg/L. Amending existing stormwater BMPs with low-cost adsorbent media could result in the improved metals removals necessary to meet impending regulations. With the limits of existing BMPs, there is an eminent need

for efficient, low-cost alternatives for the treatment of highway stormwater runoff. The current study is focused on the evaluation of a biogenic fish-bone based alternative adsorbent, Apatite IITM, for use in stormwater BMPs to improve the removal of copper.

The work described here is a part of a larger multi-year project that has been divided into three phases. Phase one included an extensive literature review and laboratory experiments aimed at understanding the mechanisms for copper removal by Apatite IITM in synthetic stormwater solutions (Huang 2012). Phase two (the work shown here) included follow-up laboratory experiments, selection of an appropriate field site, and the design, construction and installation of a field-scale filter system. Phase three is planned to utilize the constructed field-scale filter system to study the removal of copper with full-size Apatite IITM in actual highway stormwater runoff.

1.1 Objectives

As stated above, this work focuses on (1) gaining improved understanding of the mechanism responsible for copper removal with Apatite IITM in laboratory-scale experiments and (2) the design and construction of a field-scale filter system to investigate copper removal from actual highway stormwater runoff. The specific objectives of this work are to:

- 1) Characterize the equilibrium adsorption capacity of Apatite IITM for a broader range of initial concentration of copper and zinc in single-element systems;
- 2) Assess the effects of influent concentration on the removal of copper and zinc from synthetic stormwater in continuous-flow column experiments;
- 3) Identify a suitable field site with sufficient flow and dissolved copper for testing of a field-scale filter;
- 4) Design a field-scale filter system to remove copper with Apatite IITM from actual highway stormwater runoff; and
- 5) Construct and install the filter system at the field site.

1.2 Approach

The first objective was accomplished through the use of single-element batch studies. Equilibrium single-element removal capacity relationships were developed to characterize the removal of copper and zinc by Apatite IITM. Previous work developed rapid small scale column tests (RSSCT) parameters to simulate copper and zinc removal from stormwater runoff using Apatite IITM in full-scale systems (Huang 2012). Drawing on the results from the batch testing and parameters estimated for a full-scale Apatite IITM installation, RSSCTs were utilized to accomplish the second objective. Influent concentrations were varied in column experiments to assess the effects of influent concentration on copper removal. The third objective was met by visiting prospective field sites and creating a decision matrix to choose the best possible site. To confirm sufficient flow and copper loading, storm events were sampled from one site in Salem, OR. First flush and flow-paced samples were collected to characterize the stormwater quality and quantity to inform the filter design process. To approach the fourth objective, a land survey and stormwater sampling were performed to assess existing site characteristics and water quality. Data gathered informed engineering concepts that were used to optimize parameters such as flowrate and surface area of the filter bed. The optimized parameters were used to design a field-scale stormwater filter. Finally the last objective was accomplished by constructing the designed filter system and installing it at the selected field site.

The remainder of the thesis is organized as the follows: Chapter 2 describes previous work and provides a summary of literature relevant to issues related to copper in stormwater, currently employed filtration best management practices (BMPs) for stormwater runoff, and use of compost for the remediation metals in stormwater; Chapter 3 presents information on materials and methods for both laboratory and field experiments; Laboratory results are presented and discussed in Chapter 4; Chapter 5 describes field site characterization and the design and construction of a field-scale filter system; conclusions and recommendations for future work are included in Chapter 6.

2 Literature Review

2.1 Copper in highway stormwater runoff

Highway stormwater runoff is a significant non-point source of many contaminants into natural surface waters. In urban areas, metals such as Cu, Cd, Zn, Pb, Ni and Cr are commonly detected in highway stormwater runoff. Current studies have found that many of these metals are toxic to aquatic life (Kayhanian 2010, Howell 1979, Hewitt and Rashed 1988, Makepeace et al. 1995). Among the metals commonly found in stormwater, copper is of particular concern due to its toxic effects on juvenile salmon at low concentrations. Predator avoidance behavior and olfactory function of juvenile Coho salmon were inhibited at dissolved copper concentrations as low as 2 µg/L for short-term (3 hour) exposures (Sandahl et al. 2007). Additionally, exposing juvenile Coho salmon to 20 µg/L dissolved copper for 30 minutes in artificial fresh water reduced the olfactory response to a natural odorant, L-serine, by 82% (McIntyre et al. 2008). Moreover, adjusting the alkalinity, hardness and dissolved organic carbon (DOC) to levels generally found in western rivers did not significantly reduce the toxic effects.

Major sources of copper found in stormwater runoff include atmospheric deposition, vehicle emissions, building roofing, and industrial emissions (Joshi and Balasubramanian 2010, Davis et al. 2001, Kim and Fergusson 1994, Sabin et al. 2005). The most significant source of copper in highway stormwater runoff is considered to be brake pad wear (Davis et al. 2001, Moran 1997, Legret and Pagotto 1999). The concentrations of dissolved and total copper range between 1.1~130 µg/L and 1.2~270 µg/L, respectively, in highway stormwater runoff (Nason, Sprick and Bloomquist 2012, Kayhanian 2010). Dissolved copper concentrations are positively correlated with both DOC and alkalinity, and are negatively correlated with pH (Nason et al. 2012). The same study found that total copper concentrations in highway stormwater runoff positively correlate with both TSS and DOC. Copper concentrations typically

found in highway stormwater runoff are higher than the levels at which juvenile Coho salmon can be affected. Currently, the Oregon Department of Environmental Quality stipulates that total copper discharged in industrial stormwater runoff must be less than 20 µg/L (ODEQ 2012). Transportation projects deemed likely to adversely affect threatened and endangered aquatic species must adhere to biological opinions issued under section 7 of the Endangered Species Act (ESA). As such, there is an eminent need for cost-effective treatment technology that can remove dissolved copper below levels that adversely affect juvenile salmon.

2.2 Previous laboratory experiments with Apatite II™

Apatite II™ (US Patent #6,217,775), a fish-bone-derived biogenically precipitated calcium, phosphate, hydroxide mineral (Wright and Conca 2002, Krejzler and Narbutt 2003). Apatite II™ has been shown to remove zinc at greater than 99.5% at initial concentrations ranging between 44.7-146.9 mg/L in recent studies (Conca and Wright 2006, Oliva et al. 2010). Investigation of Apatite II™ performance with relevant divalent heavy metal (µg/L) and background ion concentrations commonly found in highway stormwater runoff is necessary.

The work described in this thesis builds on previous laboratory-scale experiments examining copper and zinc removal using Apatite II™ (Huang 2012). The earlier study achieved the following objectives:

- Characterized the structure and composition of Apatite II™;
- Characterized the removal of copper and zinc by Apatite II™ in single-element and dual-element batch systems;
- Evaluated the dynamic removal of copper and zinc from synthetic stormwater in rapid small scale column tests (RSSCTs); and
- Proposed mechanisms for the removal of copper and zinc by Apatite II™.

Initial studies by X-Ray Diffraction (XRD) confirmed the crystal structure of Apatite II™ was hydroxyapatite, $[\text{Ca}_5(\text{PO}_4)_3\text{OH}]$. Results from SEM-EDS found the ratio of

Ca:P:Na:C:O in the Apatite II™ to be 8.99: 5.42:1.00:54.98:39.41. Apatite II™ contained up to 30-40 weight percentage of organic material associated with the mineral phase.

The removal of copper and zinc by Apatite II™ was determined through laboratory-scale batch experiments. Batch solutions initially contained 0-6400 µg/L of copper and/or zinc in a synthetic stormwater matrix. Hypothesizing a primarily adsorption based removal mechanism, single-element (copper only and zinc only) and dual-element (copper and zinc) batch experiments were completed and the results fit to removal capacity relationships relating the removal capacities (mg Me/mg Apatite II™) of copper and zinc to equilibrium aqueous phase concentrations. Copper removal was best characterized by a linear isotherm ($K = 0.014$ L/mg). The linear isotherm takes the general form $q_e = KC_e$, where q_e is the amount of solute adsorbed per unit mass of adsorbent, K is the equilibrium distribution coefficient, and C_e is the equilibrium solute concentration. Removal of zinc was characterized by a Freundlich-type isotherm ($K_f = 0.082 \frac{\mu\text{g}^{0.287} \cdot \text{L}^{0.0.713}}{\text{mg}}$, $\frac{1}{n} = 0.836$). The Freundlich-type isotherm takes the general form $q_e = K_f C_e^{\frac{1}{n}}$, where q_e is the amount of solute adsorbed per unit mass of adsorbent, and K_f is the Freundlich sorption coefficient. Dual-element batch experiments were also carried out to examine competitive effects between copper and zinc. Zinc is another divalent cation with similar properties as copper and is commonly present at higher concentrations than copper in stormwater. As a result, zinc may affect the removal efficiency of copper in adsorptive or precipitative treatment processes. Similar to the single-element experiments, copper removal was characterized by a linear isotherm ($K = 0.013$ L/mg) and zinc was best described by a Freundlich isotherm ($K_f = 0.189 \frac{\mu\text{g}^{0.374} \cdot \text{L}^{0.626}}{\text{mg}}$, $\frac{1}{n} = 0.626$). The equilibrium relationships for copper with and without zinc were not statically different, indicating that the presence of zinc had no effect on the removal of copper. At equilibrium, large

quantities of calcium and phosphate were detected, indicating dissolution of the Apatite II™ media. Equilibrium pH in the batch experiments was 7.2-7.3.

Rapid small scale column tests (RSSCT) were performed to assess the dynamic removal efficiency of Apatite II™ in continuous-flow systems. Zinc breakthrough occurred more rapidly than copper breakthrough. Similar to the batch results, phosphate and calcium were detected at high levels in the effluent. Initially, concentrations were similar to those found in the batch experiments, but decreased over time. Even when zinc was present at 4 times the concentration of copper, it did not significantly affect copper removal. This result confirms what was observed in the batch studies. At extended times, effluent copper and zinc concentrations were greater than influent concentrations, indicating the removed metals were being released to the water. This was attributed to re-dissolution of previously deposited solids or desorption caused by decreasing pH over the duration of the tests. SEM-EDS was used to analyze the composition of Apatite II™ before and after column experiments. Copper removed from solution was detected on the Apatite II™ surface. Depleted values of calcium and phosphate confirmed the dissolution of the apatite mineral. A distinct copper phase was not detected with XRD analysis due to poor crystallinity and low relative concentration.

Conca and Wright (2006) used an Apatite II™ permeable reactive barrier to remediate groundwater containing Zn, Pb, and Cd. Apatite II™ was found to sequester metals by four different mechanisms depending on the type of metal, concentration, and aquatic chemistry. Apatite II™ was found to continuously supply phosphate, which causes the solution to exceed solubility limits of various metal-phosphate solids. At lower concentrations, precipitation can occur onto preexisting phase by heterogeneous nucleation. Transition metals can also be adsorbed onto Apatite II™ through the surface hydroxyl and phosphate groups. Precipitation can also be caused by chemical changes induced by sulfate reducing bacteria. The dissolution process of Apatite II™ releases phosphate and hydroxide, which results in the pH being buffered near neutral (Conca and Wright 2006). It was determined that the presence of phosphate was

necessary for any substantial zinc removal to occur, likely because removal was primarily achieved through precipitation of hopeite [$\text{Zn}_3(\text{PO}_4)_2 \cdot 4\text{H}_2\text{O}$] (Oliva et al. 2010). Based on the results of modeling and batch precipitation tests, zinc was found to be more soluble than copper. Large amounts of zinc were removed by the precipitation of hopeite based on modeling results (Huang 2012). The lower energy barrier required for heterogeneous nucleation may also have resulted in the formation of more hopeite in the experiments with Apatite II™. Alternatively, this result could be due to sorption of zinc onto Apatite II™ surface.

Copper removal by Apatite II™ may occur through precipitation and or surface complexation (Huang 2012). Simulation with visual MINTEQ and batch experiments without the presence of Apatite II™ were conducted to isolate the contribution of each removal mechanism. The results demonstrated that, as expected, dissolved copper concentration decreased as solution pH increased. Comparison of the results from batch tests with and without Apatite II™ suggested that more than 85% of copper was removed by precipitation for initial copper concentration higher than 400 $\mu\text{g/L}$ (Huang 2012). Other studies have proposed libethenite [$\text{Cu}_2(\text{PO}_4)\text{OH}$] as a possible copper-containing crystal phase (Oliva et al. 2011). In previous work, libethenite was considered a possible copper-related precipitate but was not shown to be thermodynamically favored at equilibrium in modeling results with visual MINTEQ (Huang 2012). Apatite II™ has many possible mechanisms for remediating metals from solution and represents a promising alternative media for use in stormwater BMPs.

2.3 Filtration based BMPs for metals removal

Filtration based BMPs including filter strips and media filters can be installed with beds of single or mixed media for treatment. The selection of appropriate media is important when optimizing for metals removal. Barrett (2005) compared the performance of several BMPs including sand filters, detention basins, multi-chambered treatment train (MCTT), biofiltration strips and vegetated swales. The

removal of TSS in sand filters was found to be independent of influent concentration, while the removal of TSS by swales and detention basins varied with inlet concentrations. With the exception of swales and detention basins, all other examined BMPs achieved more than 80% reduction of TSS at an influent concentration of 114 mg/L. Metals removal was also characterized; it was shown that removal efficiencies for zinc were generally higher than for copper. Of all the BMPs examined, biofiltration strips resulted in the greatest removal of dissolved copper (between 70~80%).

The association of total metals removal and TSS removal was investigated in field-scale wet detention ponds (Hossain et al. 2005). The field site drained approximately 10 ha of highway pavement area with an average daily traffic (ADT) of 49,400 vehicles. Automatic water samplers were used to monitor flow and collect samples from the influent and effluent over the course of 2 years. Event mean concentration were measured to characterize influent TSS (9.6-1850 mg/L), Cd (0-16 µg/L), Cu (7-209 µg/L), Pb (7-194 µg/L), and Zn (108-1267 µg/L) concentrations. The measured effluent concentration of TSS resulted in removal efficiency ranging from 68.1-99.4%. Significant removal of total metals was observed, with metals removal efficiencies between 0-100% (Cd), 20.8-99.3% (Cu), 7.1-98.7% (Pb), and 8.2-92.8% (Zn). The primary removal mechanism was found to be partitioning of metals onto solids. Consequently, total metal removal efficiency was found to correlate with TSS removal. Total metal removal efficiency of the pond was 72.5-86.9% of the TSS removal efficiencies. This is an important consideration in the design of stormwater BMPs; significantly reducing total metals concentration will reduce the amount of metals available to dissolve if a change in aquatic chemistry occurs.

Laboratory-scale batch experiments were performed to assess the removal of heavy metals with the addition on zeolites in synthetic stormwater and stormwater collected from highways (Pitcher, Slade and Ward 2004). This study was designed to help discern possible factors that influence metals removal in actual highway stormwater compared to synthetic metal solutions. Collected highway stormwater was spiked to contain similar initial metal concentrations to synthetic solutions of 25, 50, 250 and

500 µg/L of Cd, Pb, Cu and Zn, respectively. Synthetic zeolite effectively removed heavy metals in both synthetic stormwater and actual highway stormwater; the studied metals were Pb (100%, 100%), Cu (98.4%, 91.6%), Zn (96.8%, 96.5%), and Cd (100%, 100%). Highway stormwater initially contained large amounts of sodium, calcium, and magnesium as a result of de-icing salt addition. Calcium was found to compete with other metal species for ion exchange sites. Final solution pH in experiments with synthetic zeolite was increased to 8.5-9.0, due to hydronium ion exchange reducing protons in solution. Dissolved metal concentrations were reduced by increased initial pH and increased organic content complexing dissolved metals, resulting in less available dissolved metals for adsorption onto the zeolite.

A report published by the international stormwater BMP database summarized the performance of a variety of BMPs for metal abatement (Wright Water Engineers and Geosyntec Consultants 2011). All tested BMPs displayed significant reductions of total zinc. When influent concentrations ranged from 50-99 µg/L, effluent concentrations were reduced between 15 and 30 µg/L. Similar results were reported for total copper remediation. With the exception of wetland channels, most BMPs resulted in significant reductions of total copper. Bioretention ponds, bioswales, filter strips, media filters, porous pavement, retention ponds, and wetland basins were found to reduce dissolved zinc concentrations to 8-25 µg/L. Similar technologies were not as effective at removing dissolved copper. Significant removal of dissolved copper was observed in detention basins, filter strips, and retention ponds where the corresponding effluent (influent) concentrations were 4.8 (5.3), 5.3 (11.1), and 5.0 (7.5) µg/L, respectively. Reducing dissolved copper concentrations below levels that adversely affect juvenile salmon is not feasible with most currently employed BMPs. As a result, it is important to explore cost effective alternatives to improve the removal capacity of dissolved copper in current systems.

Alternatively, some studies have achieved removal of dissolved copper to concentrations below 5 µg/L at the field-scale with synthetic metal solutions. Experiments were performed to assess the removal of dissolved metals from synthetic

stormwater in a field-scale bioretention system (Davis et al. 2003). Influent heavy metals contained in synthetic stormwater were 80 µg/L (Cu), 80 µg/L (Pb), and 600 µg/L (Zn). A peristaltic pump was used to deliver the influent solution to the top of the bioretention system. Grab samples were taken from the effluent every 30 minutes. Significant removal of dissolved Cu, Pb, and Zn were achieved in the bioretention system where the corresponding effluent concentrations were 2 ± 1 µg/L, <2 µg/L, and <25 µg/L, respectively. Removal efficiency was found to improve with increasing bioretention depths. The proposed removal mechanism was adsorption of heavy metals to the surface mulch layer and soil media.

Stormwater runoff from site to site is highly variable with respect to metal concentrations, pH and other parameters. For instance, longer residence times have shown to improve removal of dissolved copper in experiments with different filter media (compost, peat-sand mix and zeolites) (Johnson 2003). Considering removal efficiency is a function of metals concentration and type, site conditions should be considered before choosing the appropriate media. When designing a treatment system, the advantages and disadvantages of each media should also be considered. Disadvantages such as compost adding color to effluent can reduce applicability of some media for stormwater treatment (Johnson 2003).

2.4 Removal of metals with compost

Compost, which is currently applied in many BMPs for storm water treatment, has been investigated by several groups (Sun and Davis 2007, Maurer 2009, Davis et al. 2003, Li and Davis 2009). Batch tests have shown that compost alone can remove 93-98% of copper, 88-96% of zinc, 97-98% of lead, and 97.9% of cadmium (Seelsaen et al. 2007, Grimes, Taylor and Cooper 1999). Once adsorbed, heavy metals were not found to leach back into solution. As a result, compost can be used in filters for an extended period of time without the possibility of contaminants re-entering the effluent storm water (Grimes et al. 1999). The ability of compost to achieve high removal

efficiencies and retain previously removed metals makes it a promising cost effective recycled media to remediate metals from highway stormwater runoff.

Clark et al. (1999) evaluated a compost filter over three years using collected storm water runoff. The greatest removal efficiency occurred during the first flush of the filter which had the heaviest pollutant loadings, showing that this type of filter is capable of handling shock loadings. During this first flush, the compost filter removed 83% of copper, 86% of zinc, 86% of lead, and 93% of iron (Clark and Pitt 1999).

Seelsaen et al. (2006) tested sand, zeolite, compost, and packing wood for their applicability to remove heavy metals typically found in stormwater. Metal concentrations 50 times typical stormwater concentrations were used to test the capacity of the tested materials. Compost and packing wood resulted in the highest removal capacity of copper and zinc. Compost removed 97% of the initial zinc and 92% of the initial copper.

Seelsaen et al. (2007) performed sorption experiments to investigate the removal of dissolved copper, zinc, and lead by use of garden derived compost. Batch studies were performed with synthetic stormwater at pH 5 with initial concentrations of copper, lead, and zinc ranging from 5 to 100 mg/L. The compost removed 93% of the copper, 88% of the zinc, and 97% of the lead with initial concentrations of 100 mg/L and 5 g of compost. Sorption efficiency of copper at a concentration of 180 mg/L increased from 88% to 97% as particle size decreased from 4,750 μm to 180 μm . As particle size decreases, removal efficiency increases due to an increase in the ratio of surface area to volume. A larger surface area allows for a greater amount of adsorption (Seelsaen et al. 2007).

Sun and Davis (2007) evaluated a bioretention system for metals removal from synthetic runoff. The bioretention system consisted of a top 5 cm layer of 50% planting soil and 50% leaf mulch, followed by a layer (5-25 cm) of 50% sand, 30% planting soil, and 20% leaf mulch. Three independent experiments were conducted in which different grass species (*Panicum Virgatum* , Kentucky-31 , and *Bromus*

ciliates) were planted on the top of the system. Results indicated that the effectiveness of metals uptake was nearly the same for different grass species. 94% zinc, 88% copper, 95% lead and > 95% cadmium were removed when the corresponding inlet concentrations were 660, 71, 67, 21 $\mu\text{g/L}$, respectively. Such high removal efficiencies were mainly by compost-amended soil (88-97%) rather than accumulating in plants (0.5-3.3%).

The removal mechanisms by compost-amended soil include soil filtration, adsorption, ion-exchange and biotransformation. More adsorption sites provided by organic matter in compost-amended soil bioretention systems results in the improvement of the effectiveness for metals remediation through adsorption processes (Sun and Davis 2007, Maurer 2009). Although relatively efficient for metals removal, compost has also been shown to leach a large amount of dissolved organic carbon (DOC). Using different mixes of compost, sand, and other sorbents can reduce the amount of DOC released while still allowing adsorption of heavy metals (Seelsaen et al. 2006).

Compost has been found to contain significant amounts of various heavy metals such as 4,196 mg/kg aluminum, 10,194 mg/kg calcium, 3,347 mg/kg iron, 3,372 mg/kg potassium, 2,593 mg/kg magnesium, 1,434 mg/kg sodium, 386 mg/kg phosphorous, 527 mg/kg sulfur, 37,221 mg/kg silicon, 40 mg/kg copper, and 62 mg/kg lead (Seelsaen et al. 2007). These values corresponded well with previous studies. Grimes et al. (1999) characterized compost as 34.1% organic material, 19.8% total carbon, 1.18% total nitrogen, 0.25% phosphorous, 0.51% potassium, 0.20% magnesium, 158.5 mg/kg zinc, 50.7 mg/kg copper, 131.0 mg/kg lead, 16.6 mg/kg nickel, 21.7 mg/kg chromium, 0.92 mg/kg cadmium. The majority of compost comes from household waste, which could include a number of different products, plant material, food waste, etc. Compost amended BMPs are a currently employed technology to remediate metals from stormwater runoff in the state of Oregon. Many studies have tested the ability of compost to remove metals at high concentration (mg/L), as a result there is a need for studies with metal concentration relevant to highway stormwater runoff ($\mu\text{g/L}$). It is necessary to compare current technology (i.e. compost) with alternative

adsorbent media such as Apatite II™ to assess advantages and disadvantages applicable to the remediation of copper in highway stormwater runoff.

3 Materials and Methods

3.1 Apatite IITM

Apatite IITM (US Patent #6,217,775), a fish-bone-derived biogenically precipitated apatite material, was purchased from PIMS NW, Inc (Figure). The as-received Apatite IITM was ground by a blender, sieved to retain the 40×50 mesh and then autoclaved and air dried before use in laboratory experiments. Apatite IITM used in field experiments was used as received and had an average particle diameter of ½". The average Brunauer–Emmett–Teller (BET) surface area of Apatite IITM was 3.54 m²/g. The crystal structure was determined by XRD and it strongly corresponds to hydroxyapatite, [Ca₅(PO₄)₃OH] (Huang 2012). The general composition of Apatite IITM is Ca_{10-x}Na_x(PO₄)_{6-x}(CO₃)_x(OH)₂ with x<1, and contains up to 30-40 weight percentage of organics within the pore structure (Conca and Wright 2006).



Figure . Apatite IITM as received from PIMS NW, Inc.

3.2 Reagents

DDI water (18.2 MΩ-cm) from an ELGA Purelab Ultra system was used to prepare synthetic metal solutions in laboratory experiments. Single-element standard solutions

for Inductively Coupled Plasma (ICP) (BDH, ARISTAR) were diluted to the desired metal concentrations for use in laboratory experiments. Puratronic grade sodium chloride (Alfa Aesar) and ACS grade sodium bicarbonate (EMD Chemicals Inc.) were used to adjust the ionic strength and alkalinity of solutions used in laboratory experiments. Laboratory experiments were conducted at pH 6.0; solutions were adjusted using 3M ACS grade sodium hydroxide or concentrated ultrapure nitric acid (Aristar Ultra). Suwannee River Natural Organic Matter (SRNOM) is a whole water NOM extract isolated by reverse osmosis. SRNOM was purchased from the International Humic Substances Society (IHSS). A stock SRNOM solution was prepared by dissolving the lyophilized powder in DDI water to a concentration of 40 mg total organic carbon (TOC)/L at pH 4, as recommended by IHSS. The solution was allowed to stir for 24 hours in the dark and then filtered through a 0.22 μm membrane filter. Final TOC concentration was assessed using a Shimadzu TOC-VWS (EPA Method 415.1). The SRNOM stock solution was stored in the dark at 4 °C.

3.3 Laboratory Experiments

3.3.1 Batch Studies

Equilibrium batch studies were conducted to assess the removal capacity and removal mechanisms of Apatite II™. Synthetic stormwater solutions tested in the batch experiments initially contained 1mM NaCl, 0.185mM NaHCO₃, 0-25000 $\mu\text{g/L}$ Cu and/or 0-35000 $\mu\text{g/L}$ Zn (Figure). The concentrations of NaCl and NaHCO₃ were chosen to simulate the ionic strength and alkalinity of highway stormwater (Nason et al. 2012). Batch experiments were performed in 125 mL high density polyethylene bottles at 20°C. 200 mg of sieved Apatite II™ was added to 100 mL aliquots of synthetic stormwater in each acid washed bottle. Bottles were placed in a tumbler for 2 days to allow solutions to reach equilibrium (Huang 2012). After reaching equilibrium, each batch was filtered through a 0.45 μm membrane filter (Millipore). Immediately after filtration, solution pH was measured and aliquots were collected for sample analysis. To reduce

contamination, aliquots for metals analysis were directly filtered into polystyrene culture tubes, acidified with concentrated ultrapure nitric acid to below pH 2, and stored at 4°C prior to measurement.

Equilibrium batch studies were also conducted with the addition of natural organic matter (NOM). Synthetic stormwater solutions tested in the batch experiments initially contained 1mM NaCl, 0.185mM NaHCO₃, 0.8 mg DOC/L SRNOM, and 0-20000 µg/L Cu. All other procedures were identical to those described above.

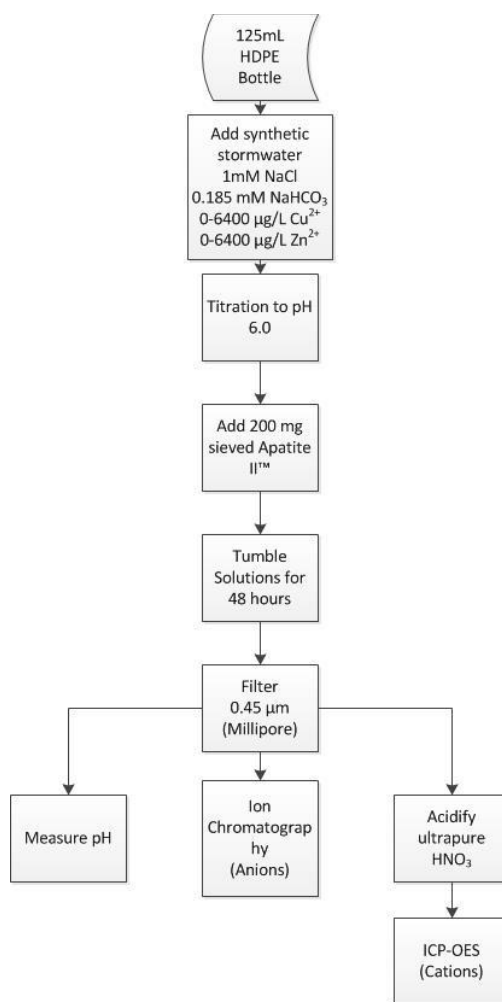


Figure . Batch experiment process diagram

3.3.1 Column Studies

Continuous flow column experiments were conducted to assess the dynamic removal capacity and breakthrough behavior of Apatite II™ (Figure). In previous work, the packed bed depth (4") was chosen as a reasonable field-scale filtration layer depth (Huang 2012). The loading rate (1 gpm/ft²) was chosen based on loading rates for exfiltration systems (Hsieh, Davis and Needelman 2007, Champagne and Li 2009, Johir et al. 2009). Field-scale characteristics were scaled down based on rapid small scale column test (RSSCT) scaling relationships (Crittenden, Berrigan and Hand 1986). A 20 cm × 1 cm Ø glass column installed with adjustable Teflon plungers (Ace Glass Inc.) was used as the vessel for the packed bed of sieved Apatite II™. Prior to experimentation, all of the column parts were rinsed with 0.1M nitric acid for 30 minutes and then subsequently rinsed with DDI water for 30 minutes before assembly. The column was then wet packed with approximately 1.82 g (4.3 cm) sieved fish bone. As shown in Figure , syringe pumps were used to pump concentrated stock solutions into a mixing chamber. The concentrated stock solutions were diluted to the desired concentrations with DI water pumped into the mixing chamber via a peristaltic pump. The mixing chamber was stirred completely before being pumped through the packed column. The influent solution contained 25-100 µg/L Cu, 1mM NaCl, and 0.185mM NaHCO₃. In dual-element experiments, 400 µg/L Zn was also included. A second syringe pump was used to adjust the influent solution to pH 6.0 before being pumped through the packed bed. Column experiments were carried out at room temperature. Samples were taken periodically at the inlet and outlet of the column in polystyrene culture tubes for measurement of pH, phosphate, calcium and copper and/or zinc.

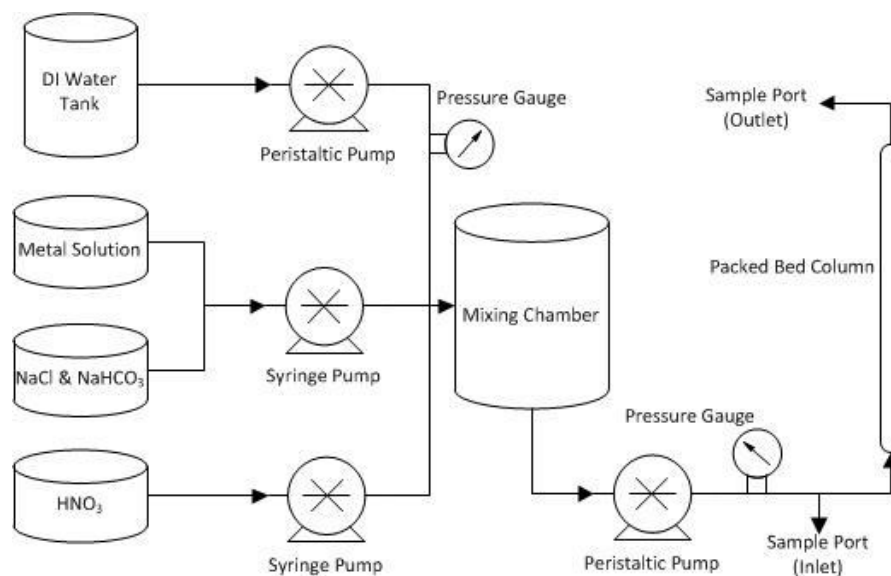


Figure . Packed bed column flow diagram

3.4 Stormwater Sampling

3.4.1 Site Description

The field site selected for this research is located on the south side of Highway 22/99E (Mission St.) near mile point 8 in Salem, OR. The annual average daily traffic (AADT) is approximately 47,400 (ODOT 2012). A system of five curbside storm drains along the south side of Highway 22 collects stormwater from the crown of the road to the shoulder. The collection system drains approximately 1.52 acres and consolidates flow to a single 12" high density polyethylene (HDPE) culvert, which eventually drains to Mill Creek. The site was primarily chosen because of its relatively high traffic, safe access, large collection area, and close proximity to Corvallis, OR. Another defining feature of the site is that it solely drains stormwater runoff. Figure , displays the aerial view of the site. The site is bounded by McNary Airfield to the southwest and Interstate 5 to the east. The star shown on the map indicates the approximate location of the 12" culvert outlet. The red box on the map outlines the drainage area.



Figure . Mission Street Aerial View

3.4.2 Sampling Equipment

An ISCO 6712 Autosampler was installed to collect flow-paced samples. Stormwater samples were collected in 24 individual 1 liter bottles. An ISCO 730 Bubbler module was connected to the autosampler to measure water level. The bubbler reported water levels to the nearest 0.001 ft. The intake line was a 25 ft long, 3/8" inside diameter Teflon tube. The intake line was connected with a Teflon coated strainer at the sample intake point. A Thel-mar combination weir was placed at the end of the 12" pipe to correlate water depth with flowrate. This created sufficient depth behind the weir to allow accurate water level measurements and collection of samples without the pump drawing air. An example of the sampling setup is shown in Figure .



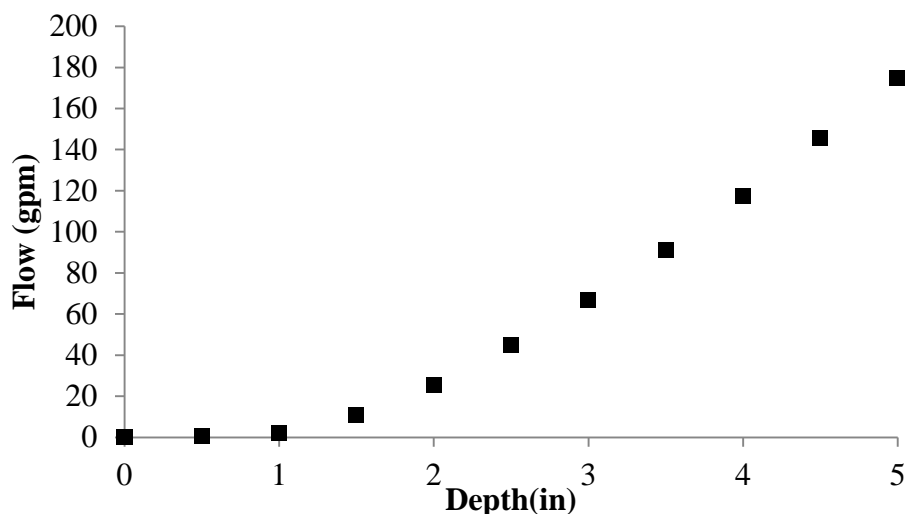
Figure . Highway 22 sampling installation

Shown in Table 1, measured flow levels were converted to flowrates using a combination weir equation (Walkowiak 2008). The Thel-mar weir is a v-notch weir for the first inch of head and then it transitions into a sharp-crested rectangular weir. Weir equations and the representative calibration curve are shown in Table 1 and Figure , respectively. An eight point calibration curve was programmed into the autosampler. Data was recorded in 1 minute intervals. ISCO Flowlink (v. 5.1) software was used to upload the data from the autosampler to a computer. The autosampler was powered by a 12 V deep cycle marine battery.

Table . Combination v-notch/rectangular weir equation

Depth (in)	Type of Weir	Equation
$d < 1$	V-notch	$Q = 1122H^{2.5}$
$1 < d \leq 5$	Rectangular	$Q = 1122\left(\frac{1}{12}\right)^{2.5} + 1495\left(L - 0.2\left(H - \frac{1}{12}\right)\right)\left(H - \frac{1}{12}\right)^{1.5}$

L is the width of the rectangular weir (8"), Q is the flowrate (gpm), and H is the head above the crest of the weir (ft).

**Figure . Calibration curve for combination Thel-mar weir**

3.4.3 Field Sampling Procedure

Prior to sample collection, the Teflon intake tubing was rinsed successively with 10% HNO₃ and DDI water. To account for headloss, sample intake volume calibration was performed in the field with DI water. The bubbler level was also calibrated in the field using DI water.

The autosampler was programmed to sample on two separate schedules: a minimum level-triggered schedule, and a flow-paced schedule. The first schedule was programmed to take one 950 mL sample when the level first measured above 0.08". This part of the program was designed to capture the "first flush" sample

from the storm. The second schedule was based only on flow-pacing and was invoked directly after the first schedule was completed. The second schedule was reprogrammed for each individual storm due to differences in stormwater volumes. The schedule was programmed by estimating the total volume of the storm (V_{total}) and dividing it by the number of samples to be taken (n). Once programmed, the autosampler can convert depth measurement to flowrate. The flowrate is then integrated and stored as total accumulated volume. The autosampler samples each time the accumulated volume reaches a multiple of the stormwater volume required to take a sample ($V_{trigger} = V_{total}/n$).

When setting up the bottle arrangement at the site, sampling bottles were handled and uncapped with nitrile gloves. After uncapping, the caps were stored in a new Ziploc bag until they were needed to reseal the bottles. After the bottle arrangement was installed, the autosampler was filled with ice to keep the samples cool during operation. Once the sampling event was stopped, the bottles were recapped with nitrile gloves. A field blank consisting of DDI water was stored uncapped with the other sample bottles in the autosampler during sampling events.

3.5 Laboratory Methods

3.5.1 Sample Fractionation

Batch and Column Experiments

All sample analysis followed the dissolved procedure shown in Figure , laboratory scale experiments focused only on the removal of dissolved metal species.

Field Experiments

Samples retrieved from the field were sealed and transported to the lab in a cooler on ice. Within two hours of collection samples were separated. Before the fractionation process, samples were completely mixed.

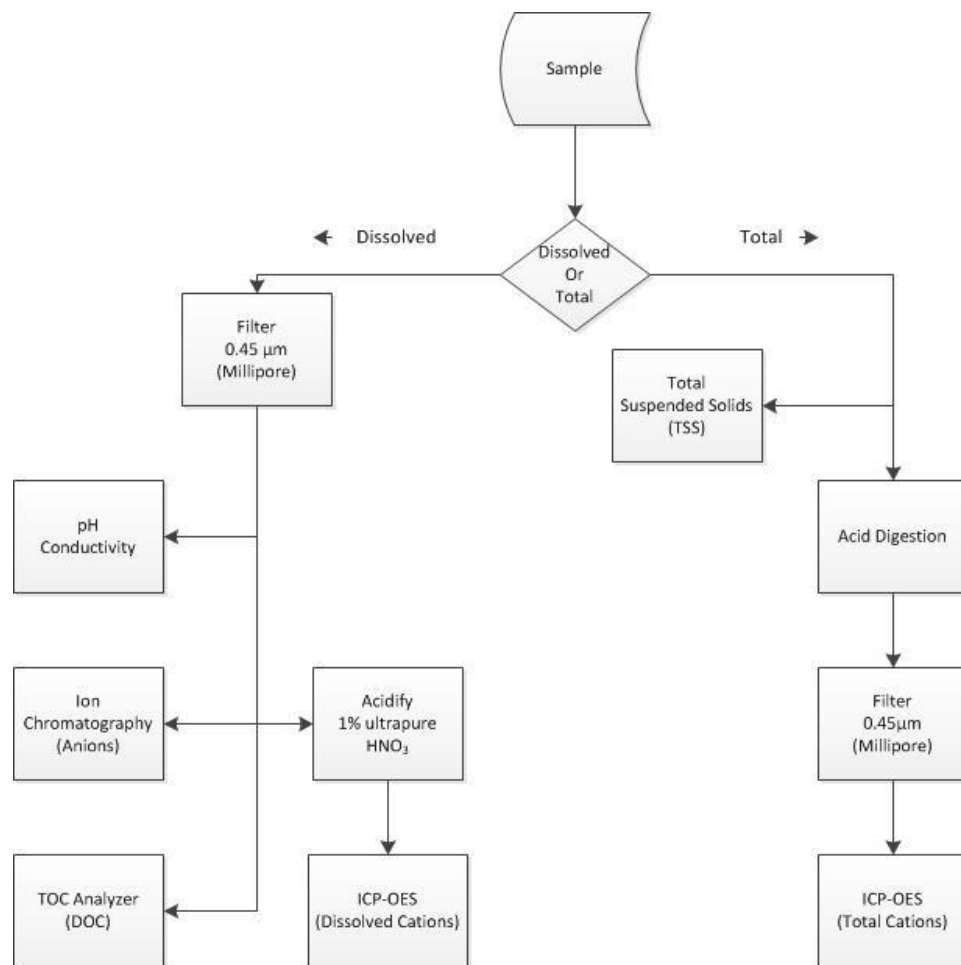


Figure . Sample Processing Flow Diagram

Once samples were returned to the laboratory, raw samples were immediately analyzed for total suspended solids (TSS). Samples were then filtered for the analyses shown in Figure , including pH, conductivity, anions, DOC, and dissolved cations. Filters (Millipore) used in the analysis were stored in 1% (v/v) ultrapure HNO₃ at least one day prior to filtration. Filters were rinsed with 250 mL of DDI water before use. Dissolved cation samples were acidified in 1% (v/v) ultrapure HNO₃ and then stored in the dark at 4°C until ICP-OES analysis. Total cation samples were separated from the bulk sample after complete mixing.

3.5.2 Total Suspended Solids (TSS)

Total suspended solids were measured in accordance with Standard Method 2540D (APHA, AWWA and WEF 2005). The total volume filtered depended on the concentration of solids in solution. Typically, aliquots of 50-100 mL of the sample were used in the filtration process. Sample analysis was performed in triplicate.

3.5.3 pH and Conductivity

Typically, 50 mL of dissolved sample was used to measure initial pH and conductivity. Initial pH was measured with a VWR symphony probe and an Accumet AR50 control panel. The pH probe was calibrated daily with pH buffers of 4, 7, and 10 (BDH General). Conductivity was measured with an Accumet conductivity probe using the same control panel. Conductivity was standardized with a 970 $\mu\text{S}/\text{cm}$ solution.

3.5.4 Cations

Total and dissolved cations concentrations were measured with Inductively Coupled Plasma Optical Emission Spectrometry (Leeman Labs Prodigy). ICP-OES was used to quantify calcium, copper, and zinc concentrations. Samples prepared for ICP-OES analysis contained 10 mL of acidified sample. Samples were stored in polystyrene culture tubes in the dark at 4°C before analysis. All samples were analyzed in triplicate. Samples for total cations, were acid digested in accordance with Standard Method 3030E.2 (APHA et al. 2005) for use with trace-level concentrations.

3.5.4 Anions

Samples were analyzed for the major anions in stormwater (nitrate, nitrite, sulfate, phosphate, and chloride) using a Dionex DX500 Ion Chromatograph. All samples were performed in triplicate. Method and standard blanks consisted of DDI water.

Standards were made for ACS grade reagents and measured along with the samples during each analysis period.

3.5.5 Dissolved Organic Carbon (DOC)

Dissolved organic carbon concentrations were determined using a Shimadzu TOC-V_{CSH} total organic carbon analyzer at Oregon State's Institute for Water and Watersheds Collaboratory. Samples were stored in the dark at 4°C prior to analysis. Samples were tested for organic carbon within a week of their receipt in the lab. Samples were typically run at a 10x dilution with DDI water. Calibration curves were constructed from standards of 0, 0.2, 0.5, 1.0, 2.0, and 5.0 mg/L of organic carbon. Standards were made at the Collaboratory with potassium hydrogen phthalate as the source of organic carbon.

3.5.6 Cleaning Procedure

3.5.6.1 General Labware

Labware used in analysis was cleaned in successive acid baths and DDI water. This cleaning procedure is detailed below:

- 1) Labware was scrubbed and rinsed with DI water.
- 2) Labware was submerged in a 10% (v/v) HCl bath for at least 18 hours.
- 3) Labware was taken out of the HCl bath and rinsed before returning to a 10% HNO₃ bath for at least 18 hours. Both acid baths were made with reagent grade acid and changed out every six months.
- 4) Upon removal from the HNO₃ bath, labware was rinsed off with DI water and submerged into a DDI bath for at least 30 minutes.
- 5) Each piece of labware was rinsed out three times with DDI water. Where applicable, containers were immediately capped after being

rinsed out. Otherwise, labware was allowed to dry upside-down and subsequently covered with Parafilm.

3.5.6.2 Organic Carbon Vials

Organic carbon vials were rinsed with DI water after use. The vials were then soaked in 10% HCl bath for at least 24 hours. After removing the vials from the acid bath they were subsequently rinsed with DDI water and allowed to hang dry upside down. As a final step, the vials were ashed in a muffle furnace for at least two hours at 550°C. The vials were then allowed to cool down and stored in Ziploc bags.

3.5.6.3 Organic Carbon Septum Caps

After use, organic carbon septum caps were rinsed DI water. The caps were then soaked in 10% HCl bath for at least 24 hours. After removing the caps from the acid bath they were rinsed with DDI water, allowed to dry and stored in Ziploc bags.

4 Laboratory Results

Building upon knowledge from previous work, further laboratory investigation of copper removal with Apatite II™ was performed. This included expanding the copper and zinc “isotherms” over a broader range of concentrations, running column experiments without the addition of a biocide, testing the ability of compost to remove copper and performing batch studies with the addition of NOM. Results and discussion of compost batch experiments are discussed in the Appendix.

4.1 Equilibrium Batch Studies

Results from single-element batch experiments are displayed in Figure . The removal mechanisms for copper and zinc in the batch experiments include precipitation, adsorption, and ion exchange. In previous work, batch tests were performed at elevated pH (7.3) with no addition of Apatite II™ resulting in similar removal efficiencies (Huang 2012). The primary removal mechanism of copper with Apatite II™ was found to be precipitation. Equilibrium liquid and solid phase concentrations are shown in Figure as removal capacity relationships where “ q_e ” represents the sum of adsorbed and precipitated metals normalized by the initial mass of Apatite II™. Similar to previous work, the removal of copper was best described by a linear isotherm ($K=0.0131$ L/mg) even after expanding the initial concentrations to 25,000 $\mu\text{g/L}$ from 6,400 $\mu\text{g/L}$ (Huang 2012). Differing from previous work, the removal of zinc was best described by a Langmuir-type isotherm ($K=0.00143$, $q_{max}=21.775$). The initial concentrations of zinc tested were expanded to 35,000 $\mu\text{g/L}$ from 6,400 $\mu\text{g/L}$ (Huang 2012), resulting in the discovery of the removal capacity approaching a maximum (q_{max}). At large initial zinc concentrations decreased equilibrium concentrations of phosphate were detected, resulting in decreased equilibrium pH. The decreased equilibrium pH would result in increased solubility of zinc-related solids. This may explain why the zinc isotherm approaches a maximum removal capacity at large initial zinc concentrations. Typically, the tendency for metal cations to sorb to oxide surfaces is highly correlated with the tendency to undergo hydrolysis and Cu^{+2} has a higher

tendency to sorb than Zn^{+2} . However, at equilibrium concentrations (C_e) less than 1000 $\mu\text{g/L}$, the removal of zinc exceeds copper. This may occur because the various copper-related solids forming in solution are more soluble than the zinc-related solids forming.

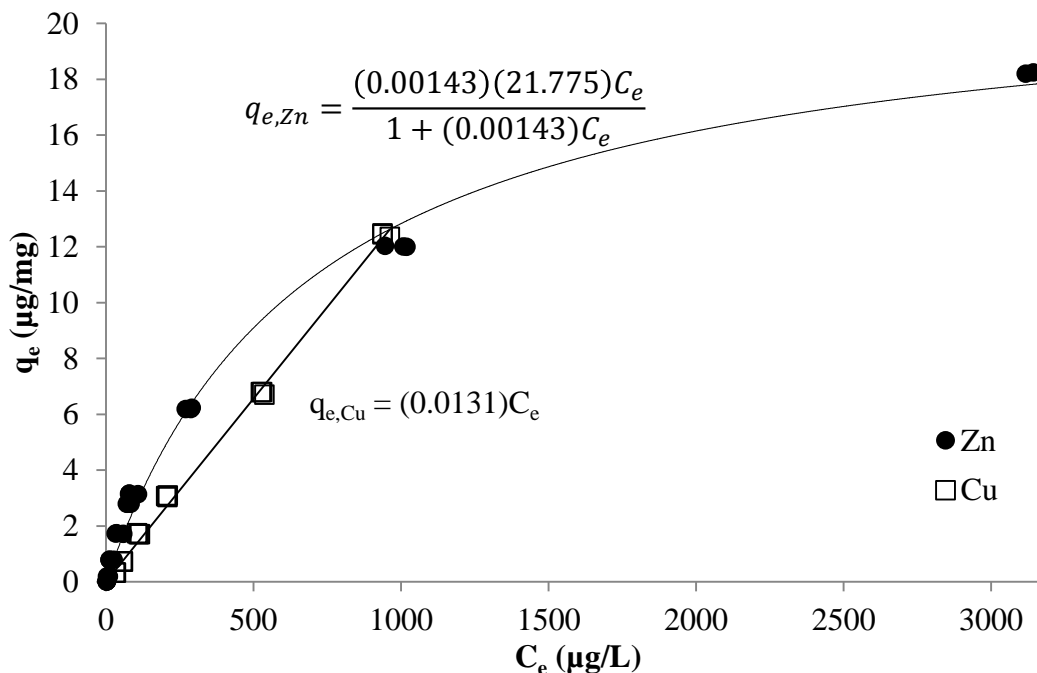


Figure . Copper and zinc removal in single-element batch studies (final pH 7.0-7.7)

Evidence of the dissolution of the apatite mineral can be seen by the large release of calcium and phosphate at equilibrium (Table 2). The final pH at equilibrium in the batch experiments was 7.0-7.7. This corresponds well with results from previous work indicating that the release of phosphate from Apatite II™ buffered the solution pH of acid mine drainage to near neutral (Conca and Wright 2006). Previous work measured equilibrium pH of similar batch studies to be between 7.2-7.3 (Huang 2012). The difference between final pH in batch experiments performed in this study and previous work is most likely due to precipitation of metal oxides resulting in the release of protons, the final pH decreased with increasing initial dissolved metal concentrations.

Table . Average pH, phosphate, and calcium at equilibrium in batch studies

	Copper	Zinc
pH	7.48 ± 0.17 ^a	6.99 ± 0.11
Average PO ₄ ³⁻ (mg/L)	24.39 ± 1.85	19.96 ± 2.28
Average Ca ²⁺ (mg/L)	9.42 ± 3.78	11.17 ± 3.50

^a95% confidence interval

Phosphate acted as a pH buffer, keeping pH elevated in the batch tests and promoting precipitation of copper solids. Previous studies indicate malachite [Cu₂CO₃(OH)₂] as the only copper-related solid phase present after comparing experimental data and modeling results with visual MINTEQ (Huang 2012). Substantial removal of copper in absence of phosphate indicates that copper-related solids formed may be non-phosphate containing solids. It was hypothesized that phosphate does not directly participate in the formation of copper phosphate solids, but when present it buffers the solution at elevated pH where the solubility of copper oxide/hydroxide solids is decreased, achieving greater copper removal. As expected, the concentration of dissolved copper increased with decreasing pH. Previous studies have proposed another possible copper-containing crystal phase libethenite [Cu₂(PO₄)OH] (Oliva et al. 2011). Alternatively, libethenite was considered a possible copper-related crystal phase in modeling with visual MINTEQ but was not shown to be thermodynamically favored at equilibrium (Huang 2012).

Previous work determined, the presence of phosphate was necessary for any substantial zinc removal to occur, likely because removal was primarily achieved through precipitation of hopeite [Zn₃(PO₄)₂·4H₂O] (Huang 2012). This behavior was previously predicted by Oliva et al. (2010). The removals of copper and zinc were greater in the presence of Apatite IITM, suggesting that adsorption and/or ion exchange is also playing a role. The presence of Apatite IITM may have also resulted in more precipitation due to the lower energy barrier required for heterogeneous nucleation. The average equilibrium phosphate concentration was lower in the zinc experiments. A possible explanation is the process of hopeite formation which consumes dissolved

phosphate. A decrease in equilibrium phosphate would cause the buffering capacity of the solution to be reduced, which resulted in decreased equilibrium pH.

Equilibrium batch studies were performed with the addition of NOM (0.8 mg DOC/L) to assess the effect of NOM on the removal of copper with laboratory-scale Apatite II™. This experiment was designed to help understand the practical implications of copper removal with Apatite II™ in the presence of NOM at the field-scale. Results from single-element batch experiments with the addition NOM are displayed in Figure . The removal of copper in the presence of NOM was best described by a linear isotherm ($K=0.0105$ L/mg). The removal of copper with Apatite II™ in the presence of NOM was inhibited. One possible explanation could be that the copper complexed with NOM, inhibiting heterogeneous nucleation (Benjamin 2010, Liu, Zhang and Talley 2007).

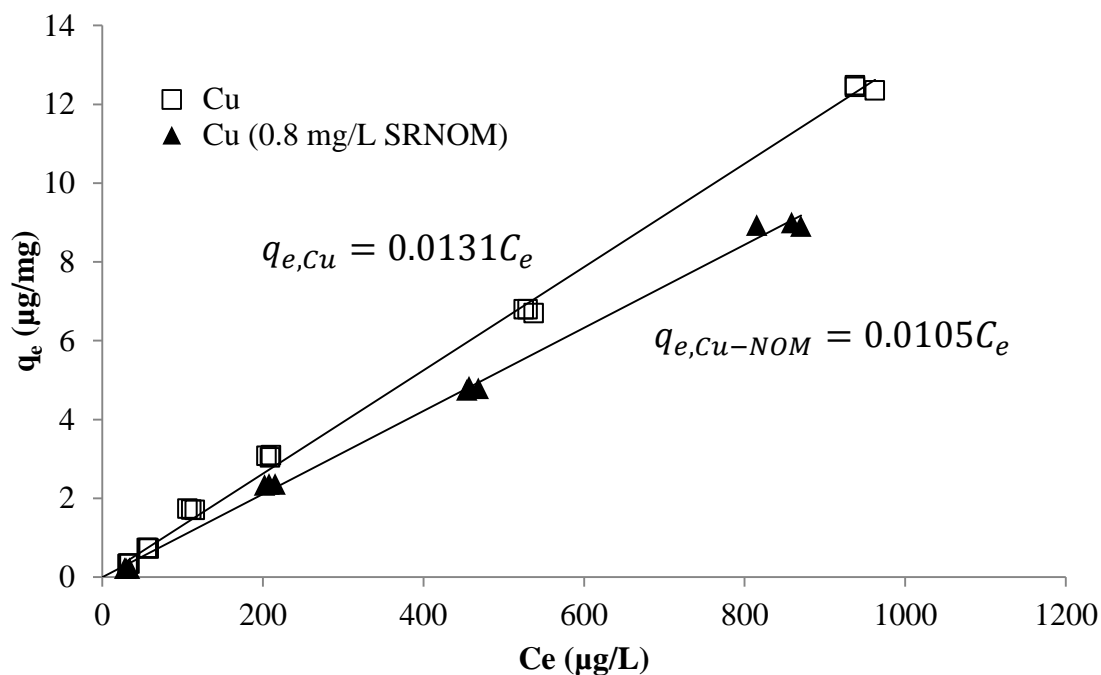


Figure . Single-element batch studies with the addition of NOM (final pH 6.6-7.0)

Equilibrium pH in the NOM test was decreased compared to previous experiments without the addition of NOM (Table). Phosphate released from the dissolution of

Apatite II™ remained the same with the addition of NOM. Calcium was not measured for the experiment with the addition of NOM. Further investigations of increasing NOM concentration are necessary to better understand field-scale filter operation. From these results it is clear that the presence of NOM in highway stormwater runoff with negatively affect the removal efficiency of copper with Apatite II™.

Table . Average pH, phosphate, and calcium at equilibrium in batch studies with NOM

	Copper	Copper (0.8 mg/L SRNOM)
pH	7.48 ± 0.17 ^a	6.85 ± 0.11
Average PO ₄ ³⁻ (mg/L)	24.39 ± 1.85	25.00 ± 2.99
Average Ca ²⁺ (mg/L)	9.42 ± 3.78	*not measured

^a 95% confidence interval

4.2 Column Studies

Previous work (Huang 2012), used RSSCTs to assess the removal efficiency of copper and zinc by Apatite II™. In the majority of those experiments, a biocide (NaN₃) was added to prevent suspected biological growth in the column experiments that resulted in sudden increases in operating pressure to an unacceptable point (>30 psi). In the tests performed with the addition of sodium azide, the time to breakthrough was shortened by approximately a third. Previous conclusions were that the difference in time to breakthrough could be explained by biologically mediated removal of copper (Huang 2012). However, the primary mechanism that has been reported in the literature involves sulfate reduction (Conca and Wright 2006) and because no sulfate was fed to these columns and the water was well oxygenated, this mechanism is unlikely. This study further investigated the subject and found that the difference in time to breakthrough could be explained by the increased ionic strength when sodium azide is present in solution. The increase in ionic strength increases copper and zinc solubility, a fact confirmed by modeling with visual MINTEQ. This effect is relevant to practical implications because of the increased ionic strength of stormwater found in areas where de-icing road salts are implemented.

Two column experiments were performed with different average influent metal concentrations, one containing only copper (37 $\mu\text{g/L}$) and the other containing copper (122 $\mu\text{g/L}$) and zinc (477 $\mu\text{g/L}$). Breakthrough curves of copper and zinc in two column experiments are shown in Figure and on a relative basis (C/C_0) in Figure . Effluent phosphate, calcium, and pH are displayed in Figure , Figure , and Figure , respectively. Comparing the copper breakthrough profiles in the single-element and dual-element column experiments indicates that zinc does not influence copper removal; this is in agreement with conclusions from previous studies (Huang 2012). In the dual-element experiment, zinc reaches breakthrough before copper (Figure). This is contrary to the behavior observed in the batch studies considering zinc has a larger removal capacity than copper at the concentrations tested in the column experiments. Zinc begins to exit the column at approximately 25 hours (Figure), at about the same time effluent phosphate concentrations severely decrease (Figure). If the primary removal mechanism for zinc is the formation of zinc-phosphate solids, the reduced availability of phosphate after 25 hours may decrease the formation of zinc-phosphate solids. When comparing the copper results in the column experiments on an absolute basis (Figure), it is evident that copper breakthrough is independent of influent concentration. As discussed previously, the precipitation of copper-related solid species is primarily a function of solution pH. Copper solids increase in solubility as pH decreases. As shown in Figure , the effluent pH over the duration of the experiment is similar in both column experiments. As a result, effluent copper concentration was the same in both column experiments. The fact that the effluent concentrations of copper are the same in the two experiments with varying influent concentrations are consistent with the breakthrough of copper being controlled by the solubility of previously deposited copper precipitates. Having the ability to treat varying concentrations of copper in stormwater runoff, becomes a very useful property of copper removal with Apatite II™. As shown in Figure , in the experiment with an influent concentration of 37 $\mu\text{g/L}$ the relative concentration exceeds 1 and previously deposited copper precipitates dissolve or desorb to maintain equilibrium with the

solubility of the copper-related solids. This results in the same measured effluent copper concentration in both experiments (Figure). This is additional evidence that effluent copper concentration is function of solution pH.

Phosphate and calcium were both detected in the effluent as a result of the dissolution of the apatite mineral. Initially, phosphate and calcium concentrations were similar to those measured in the batch experiments. Both species decreased over time, suggesting that the rate of Apatite IITM dissolution decreased over the duration of the experiment. Effluent pH also decreased over the duration of the experiment, due to decreasing concentrations of phosphate and calcium. Simultaneous release of OH⁻ occurs during the dissolution of the apatite mineral, which raises the pH. Phosphate acts as a weak acid and buffers the pH near its pKa of 7.2.

Column experiments were stopped due to an increase of pressure to maximum operating pressure of the glass column (>30 psi). This sharp increase in pressure is thought to be a result of the void space in the packed bed being filled up with metal precipitates. This can be visually seen by the packed bed changing color from the yellow Apatite IITM media to a patina (Figure).



Figure . Sieved Apatite IITM media before (left) and after column experiment (right)

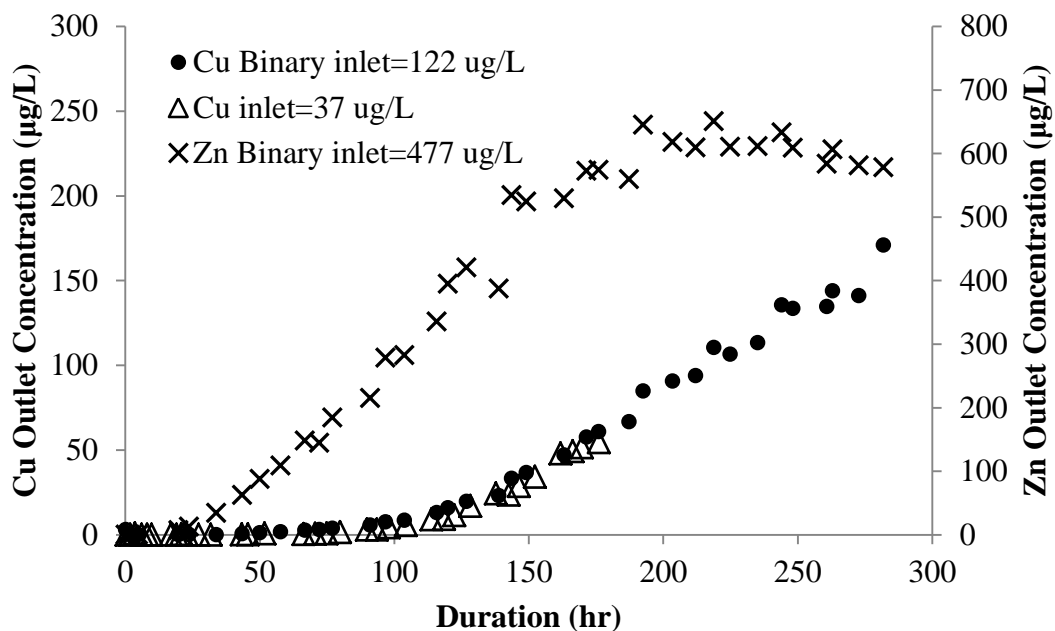


Figure . Breakthrough of copper and zinc in column experiments

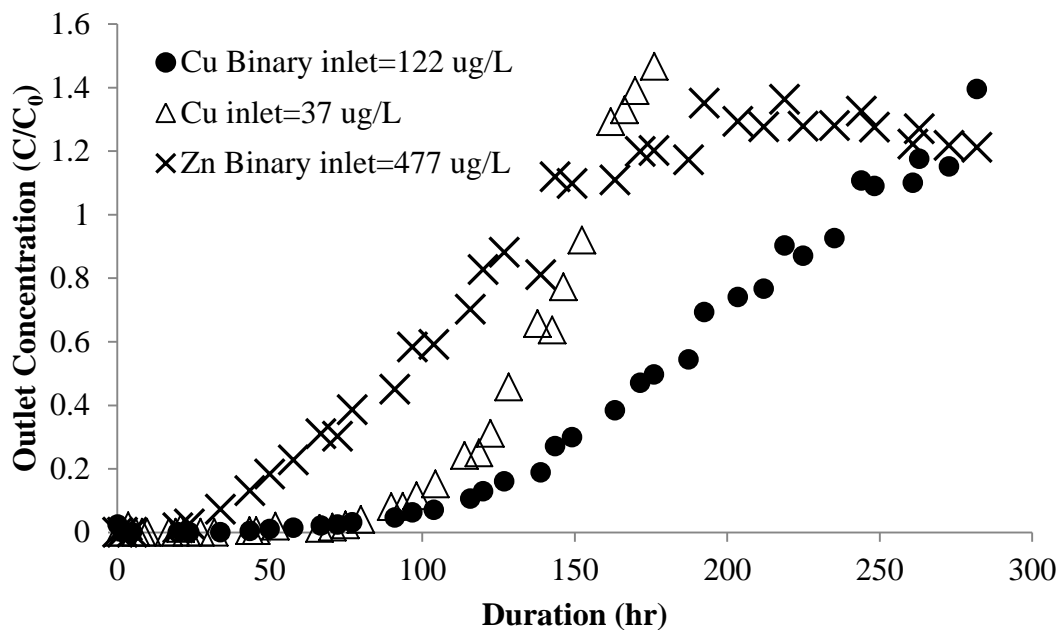


Figure . Relative Breakthrough (C/C_0) of copper and zinc in column experiments

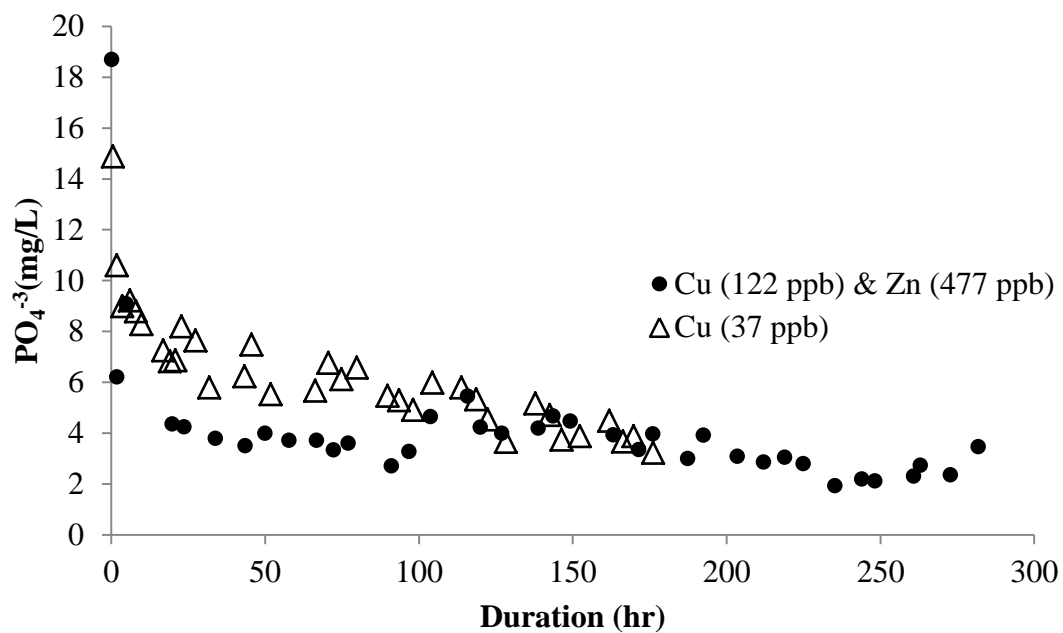


Figure . Effluent phosphate during column experiments

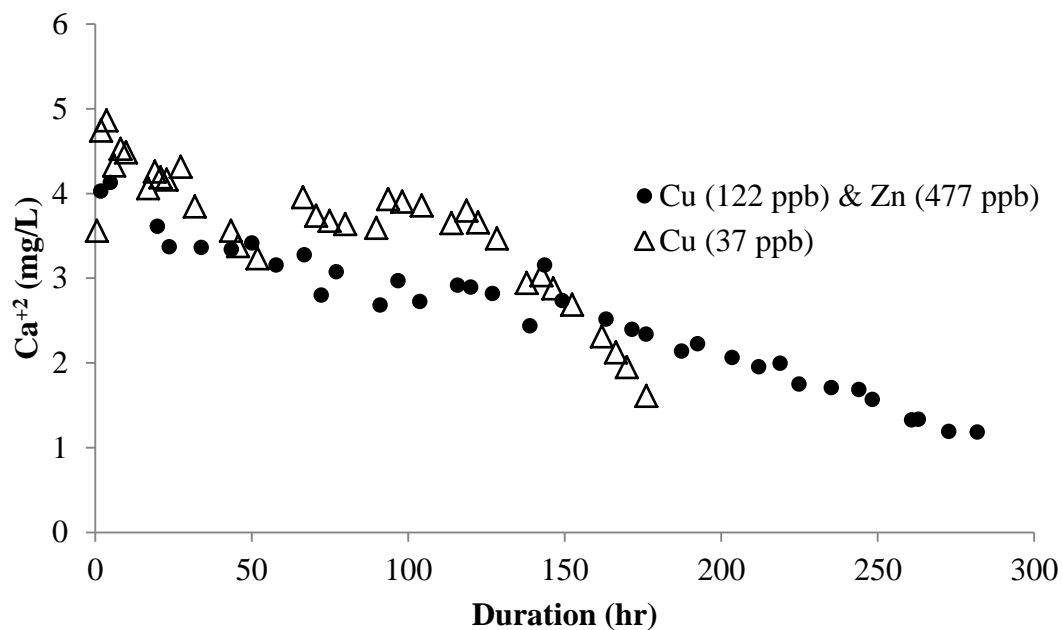


Figure . Effluent calcium during column experiments

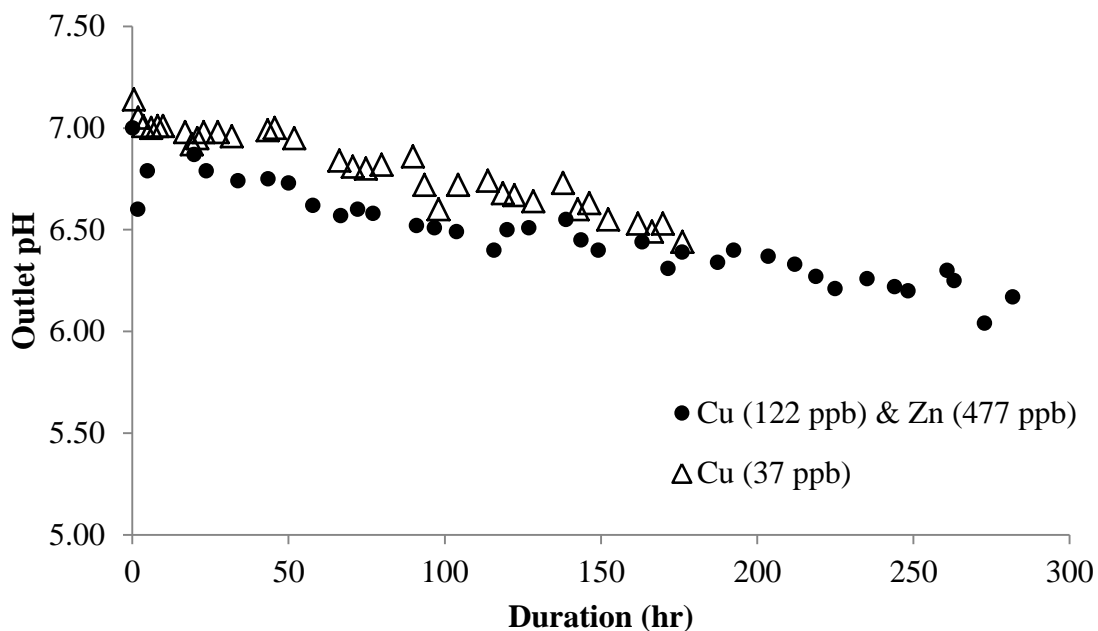
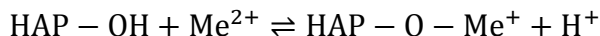


Figure . Effluent pH during column experiments

Apatite IITM performed well for continuous copper removal in both experiments (Figure). The effluent copper concentrations exceeded influent concentrations at extended durations. This likely occurs due to re-dissolution of previously filtered precipitates or desorption caused by the decreasing pH with duration (Figure). Many metal-containing precipitates are more soluble at lower pH. Moreover, surface complexation reactions like the one shown here:



would shift to the left as the concentration of protons increases. In other words, desorption is favorable at low pH. In terms of full-scale application, the release of previously deposited metals in the column experiments is a major drawback.

Monitoring the effluent metal concentrations so that the exhausted media (Apatite IITM) could be removed and replaced before metals start to release is important.

The comparison of breakthrough and removal capacities calculated based on the results of column and batch tests is shown in Table 4. Effective removal capacities in

the column tests were calculated based on the mass of metal accumulated in the column per unit mass of media at breakthrough. For the purposes of comparison with results from the batch tests, breakthrough was defined as the time when $C_{out}/C_{in} = 0.5$, which should correspond to the breakthrough of a column that rapidly reaches equilibrium between the liquid and solid phases and has no mass transport limitations.

Table . Comparison of removal capacities calculated from the column and batch experiments

	Copper	Copper and Zinc	
		Cu	Zn
$q_{e, effective}$ (from column studies) ($\mu\text{g}/\text{mg}$)	1.1	4.7	9.0
$q_{e, equilibrium}$ (from batch studies) ($\mu\text{g}/\text{mg}$)	0.5	1.6	8.8

In all cases, the removal capacities of Apatite IITM for copper and zinc in column tests were higher than those in batch tests. Some hypotheses for this behavior are discussed here. During column operation, constant influent concentrations were maintained and as a result the driving force for precipitation ($C - C_{sat}$) remains at an elevated state. Whereas in batch experiments the concentration decreases over the duration and results in decreasing driving force for precipitation over time. Furthermore, the lower energy barrier required for heterogeneous nucleation may also have resulted in more copper precipitation in tests with Apatite IITM; the differences in the solid to liquid ratio within the column and the presence of precipitated copper solids may have enhanced the precipitation process. The surface area to liquid ratio is approximately 500 times larger in the column ($18 \text{ m}^2/\text{L}$) compared in the batch experiments ($0.03 \text{ m}^2/\text{L}$). This would result in increased available surface area for heterogeneous

precipitation or crystal growth on the surface of the media. Finally, it is possible that the pH at the inlet portion of the column was significantly higher than that achieved in the batch tests and contributed to higher removal capacities through enhanced precipitation at the higher pH. This may occur because of increased dissolution of Apatite II™ near the inlet, resulting in increased phosphate which would increase the pH.

4.2.1 Estimation of bed life at full-scale

To move closer to a prediction of the estimated design life of Apatite II™, the 185th and Cornell Road expansion of the Sunset Highway in Washington County was used as the basis for a hypothetical design. For the purposes of this calculation, it was assumed that 4 in. of Apatite II™ media (ground to 0.84 mm) was placed in the bottom of the media filter drain (MFD) as shown in Figure . On the basis of design drawings provided by ODOT, the roadway is 60 ft. wide and the portion of the MFD that would contain Apatite II™ is 6 ft. wide. Based on historical records, the average yearly rainfall in Beaverton is 39 inches (<http://www.wrcc.dri.edu/cgi-bin/cliMAIN.pl?or0595>). Together, these metrics result in the required treatment of 32.5 ft³ of stormwater per ft² of Apatite II™ media (4 in. deep) per year (9.92 m³/m²-yr). Using a conservative estimate of 100 µg/L copper in the stormwater and a conservative acceptable effluent concentration of 1 µg/L, the media would be expected to treat 670 m³ of stormwater/m² of media before effluent concentrations exceeded the limit. This specific volume of stormwater treated results in a bed life of approximately 67 years. Details of this calculation are included in the Appendix. This design would involve the installation of approximately 67 lb of Apatite II™ per linear foot of roadway (one direction). According to the PIMS NW website (supplier of Apatite II™), the minimum cost (not including shipping and handling) is \$0.34/lb, which would result in a materials cost of \$22.75 per linear foot of roadway. Of

course, it is likely that the quantity of Apatite II™ installed could be substantially reduced on the basis of the estimated bed life calculated above.

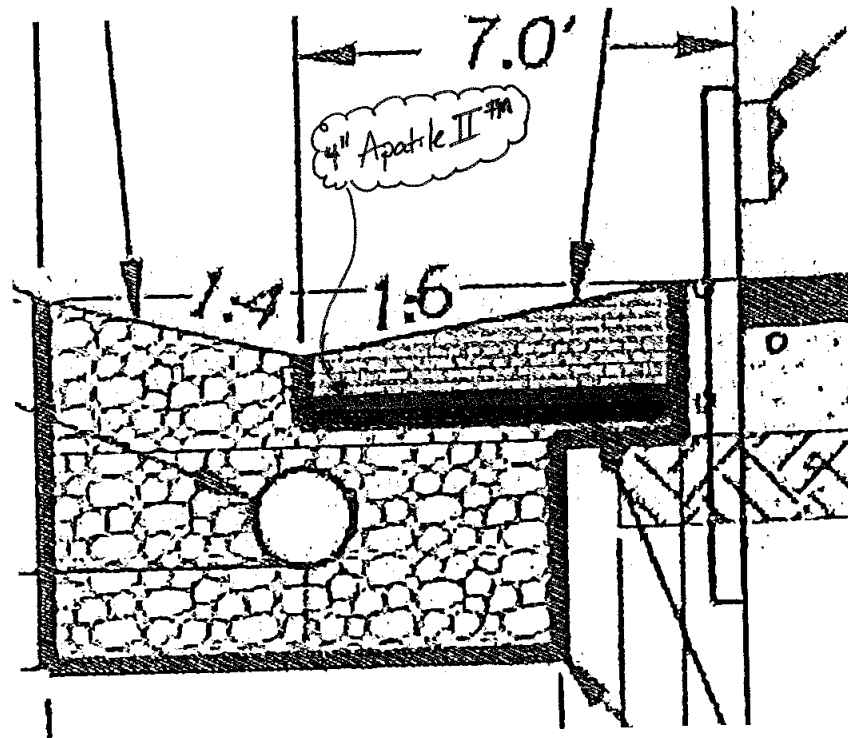


Figure . Hypothetical design incorporating Apatite II™ into a media filter drain

Admittedly, there are several assumptions in these calculations (e.g., a relatively high and constant flow rate of stormwater, relatively small media size, no effects of intermittent operation, no long-term effects of clogging). Some of the assumptions are conservative. It is possible that lower flow rates typical of stormwater runoff would also prolong bed life due to increased detention times in the packed bed. On the other hand, the use of larger (unground) media and possible detrimental effects of intermittent operation and/or clogging would reduce bed life. The extent of these effects is currently unknown and requires additional testing.

As shown in the results of both batch and column tests, Apatite II™ releases a large amount of phosphate (~20 mg/L). Phosphate release from Apatite II™ is of

concern because phosphate is a nutrient for algae and can cause eutrophication when discharged to aquatic systems. To avoid stimulation of plant growth the United States Environmental Protection Agency (USEPA) recommends that phosphate levels be kept below 0.1 mg/L. In terms of impairing receiving waters, the magnitude of the impact would be dictated by the volume water treated at a given site. As with copper removal, it is unclear how the intermittent operation of the system would influence phosphate release. It is possible that the use of mixed media containing materials designed to sequester phosphate could be used to mediate this release. However, it is noted that the release of phosphate is a key factor in the removal of both copper and zinc, a fact that must be considered in devising possible configurations (i.e., the phosphate sequestration would have to occur after the Cu removal process).

5 Field Site Design and Construction

After characterizing the ability of Apatite II™ to remove copper in the laboratory, the decision was made to pursue a field-scale investigation. This included choosing a suitable site, investigating site characteristics, stormwater sampling, and the design and construction of a field-scale filter to remove copper from actual highway stormwater runoff.

5.1 Site Selection

To help narrow down the search for a field site that would promote a successful research environment, a list of desirable site characteristics was compiled. As shown in Table , the list was broken up into necessary, desired, and optimal site qualities.

Table . Field site selection characteristics

Site Qualities	Necessary	Desired	Optimal
Safe access to sampling	x	x	x
Ability to emplace Apatite II™	x	x	x
Distinct influent and effluent locations	x	x	x
High volume AADT road		x	x
Ability to measure flow and rainfall		x	x
Close to laboratory		x	x
Secure location			x
Collects only highway runoff			x
Newer infrastructure			x

Coordinating with Oregon Department of Transportation (ODOT), a select few sites meeting these characteristics were visited. After visiting these sites, the decision was made to move forward with the site along Highway 22 in Salem, OR (Figure). Of the desired characteristics the Salem site met every one with the exception of proximity to the laboratory.



Figure . Existing ground at Highway 22 site (Salem, OR)

Some of the most desirable characteristics of this site were the large drainage area and its singular outlet point to one 12" HDPE culvert. The site also offers a safe work environment with no features within traffic lanes. McNary Field Airport was located next to the site and has a NOAA Quality Controlled Local Climatological Data (QCLCD) Weather station installed. The station (NOAA 24232/SLE) has quality controlled hourly rainfall data usually available two days after the desired date. The drainage infrastructure at the site exclusively drains water from Highway 22. The existing ground at the site had 1' of available hydraulic head between the outlet and the creek. Construction at the site was constrained to roughly 20' x 20'. Along with road debris, leaves and other plant material are heavily deposited on the road surface. These leaves were considered to be a possible problem that may induce filter clogging.

5.2 Estimating Stormwater Runoff

After choosing a suitable site, the next step was to estimate a typical storm at the site including rainfall, stormwater volume and flow. Hourly rainfall data was downloaded from NOAA's webpage from the local weather station at McNary Field. After looking

back at recent years, the month of December in 2010 had a significant amount of rainfall (9") and was chosen as a conservative estimate of what to expect for rainfall at the site. The flow exiting the 12" culvert was estimated using the rational method (Mays 2005).

$$Q = cIA \quad (\text{Eq. 5-1})$$

Where Q is the runoff flowrate (ft^3/s), c is the runoff coefficient (unitless), I is the rainfall intensity (in/hr), and A is the drainage area (acres). Flowrate was calculated by inputting, the rainfall intensity from the rainfall data, a runoff coefficient of 0.9 for concrete pavement (Mays 2005), and the measured drainage area of 1.52 acres.

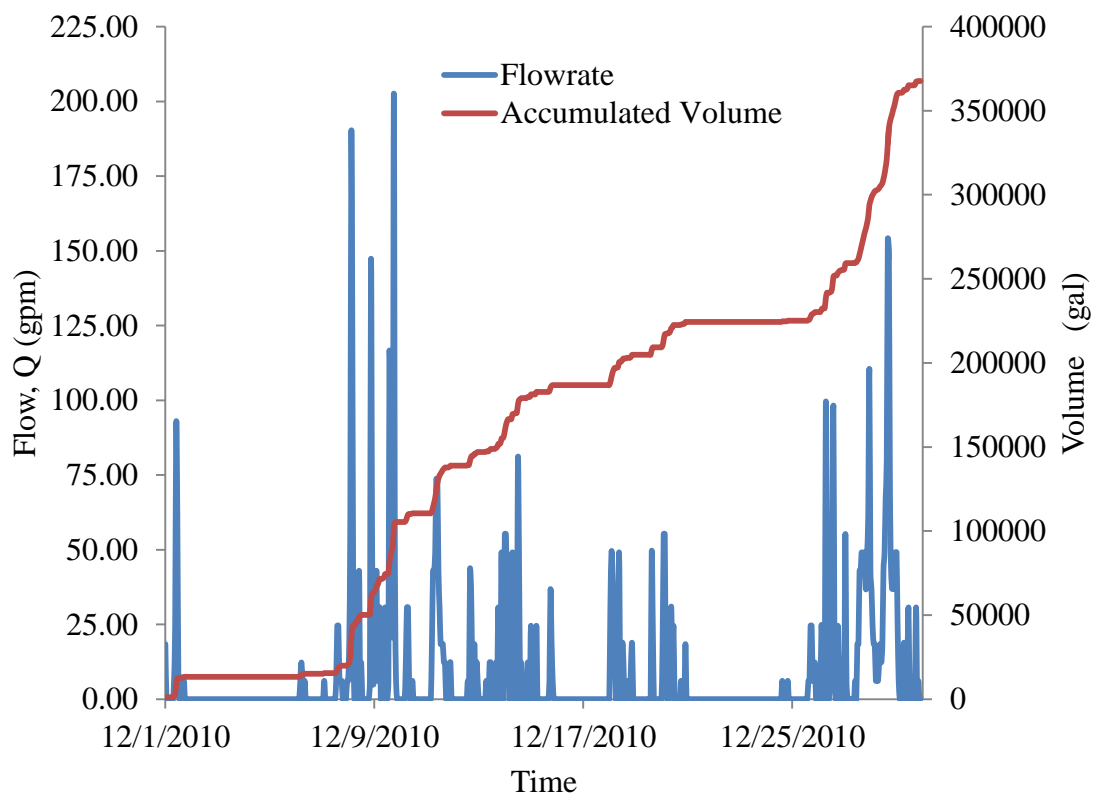


Figure . Estimated flowrate and accumulated volume during December 2010

The resulting flowrates and accumulated volumes in Figure were used to choose a surface area of the filter bed. The surface area of the filter bed was chosen to treat a

constant small portion of the total flowrate at the site and optimized to breakthrough within a reasonable amount of time. The small portion of the total flowrate was chosen to limit the hydraulic loading rate to 1 gpm/ft² as discussed in section 3.3.1. The filter bed was designed to allow for easy manipulation of variables thought to control removal efficiencies. These variables include depth of the Apatite II™ layer, depth of the filter media submerged, and hydraulic loading rates.

Filter bed surface area was varied to optimize hypothetical volume to breakthrough. Volume to breakthrough was optimized to assess filter performance over the course of multiple storms but reach breakthrough in a reasonable amount of time (<30 days of rain). Using dynamic removal capacity data from laboratory-scale testing, the volume to breakthrough ($C/C_0=1$) was estimated from the mass of Apatite II™ within the filter bed. Once the volume to breakthrough was calculated, the time to breakthrough was estimated from the volume treated through the system. Equation 5-2 was used to estimate volume to breakthrough.

$$V_b = \frac{(m)(q_e)}{C_e} = \frac{(\rho_B * V_{filter})(q_e)}{C_e} \quad (\text{Eq. 5-2})$$

Where V_b is the hypothetical volume to breakthrough (L), m is the mass of Apatite II™, q_e is the removal capacity ($\mu\text{g}/\text{mg}$), C_e is the average influent concentration ($\mu\text{g}/\text{L}$), ρ_B is the bulk density of Apatite II™ (mg/L), and V_{filter} is the volume of the Apatite II™ layer (L). The average influent concentration (C_e) and corresponding removal capacity (q_e) were chosen arbitrarily because they scale linearly (copper was fitted with a linear isotherm). After optimization, it was evident that treating the entire flow would result in unmanageable filter size. The decision was made to size the filter bed to treat a small portion of the full stormwater flowrate. The surface area of the filter bed was chosen to be 16 ft² (4'x4') to maintain a maneuverable size and to ensure constructability. As outlined above, the design hydraulic loading rate was chosen to be 1 gpm/ft². This was chosen to hold the empty bed contact time constant for Apatite II™ to remove the copper. As shown in Figure , if treating the entire flow from storms in December 2010, the actual hydraulic loading rate would vary between

0 and 13 gpm/ft², indicating that a hydraulic control structure would be necessary to limit the hydraulic loading rate to a maximum of 1 gpm/ft².

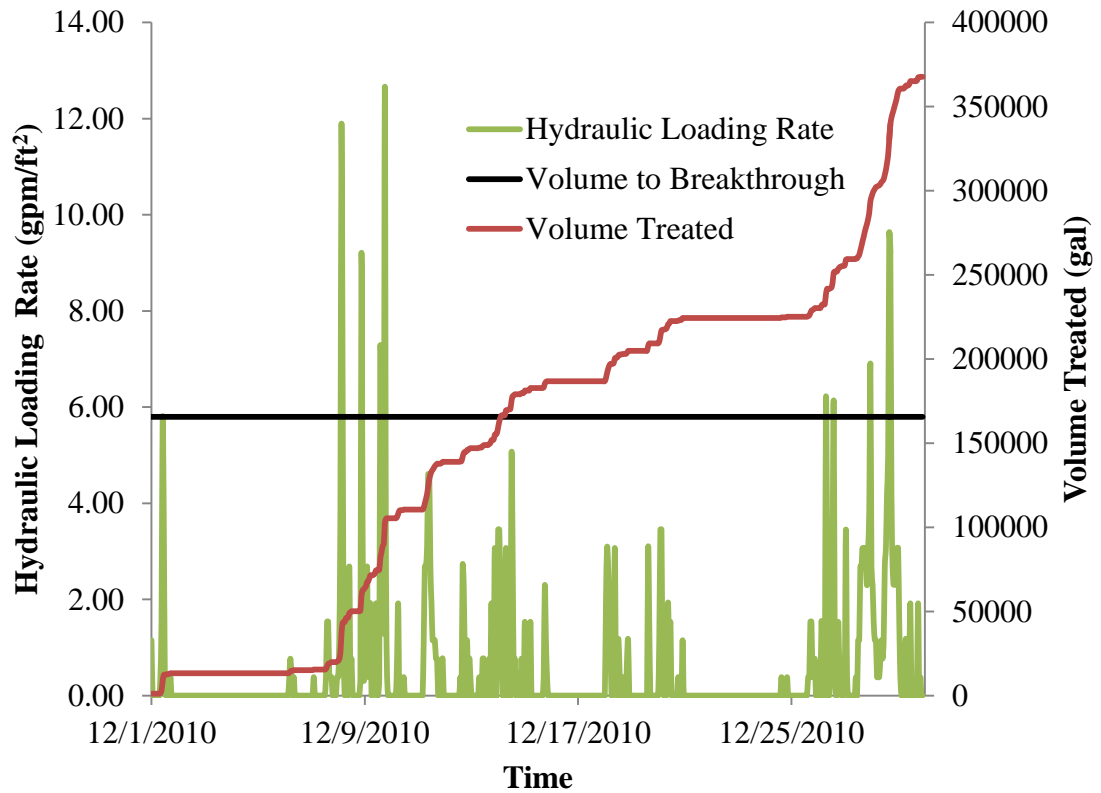


Figure . Hypothetical volume to breakthrough for 4' x 4' filter bed, hydraulic loading rate (HLR), and volume treated (full flow) during December 2010

5.3 Stormwater Sampling

After modeling flow at the site indicated sufficient flow, the next step was to monitor actual storm flowrates and water quality parameters. As explained in section 3.4.2, when taking flow-paced samples it is necessary to program the sampling event V_{trigger} . To get an estimate of the storm volume, an estimate of future rainfall was retrieved 12 hours prior to the sampling event from weather.noaa.gov. Using Eq. 5-1, flowrate and accumulated volume were calculated for the projected storm.

From this calculation, the total volume was divided by the number of samples taken (24) to calculate the volumetric interval between samples. As shown in Figure , the total storm volume was 15,473 gallons. This corresponded to taking a sample every 644 gallons. As a precaution, $V_{trigger}$ was reduced to 500 gallons to ensure an adequate number of samples. As shown in Figure , the field sampling equipment was setup at 11:00 PM on 3/4/2013 prior to the storm event.

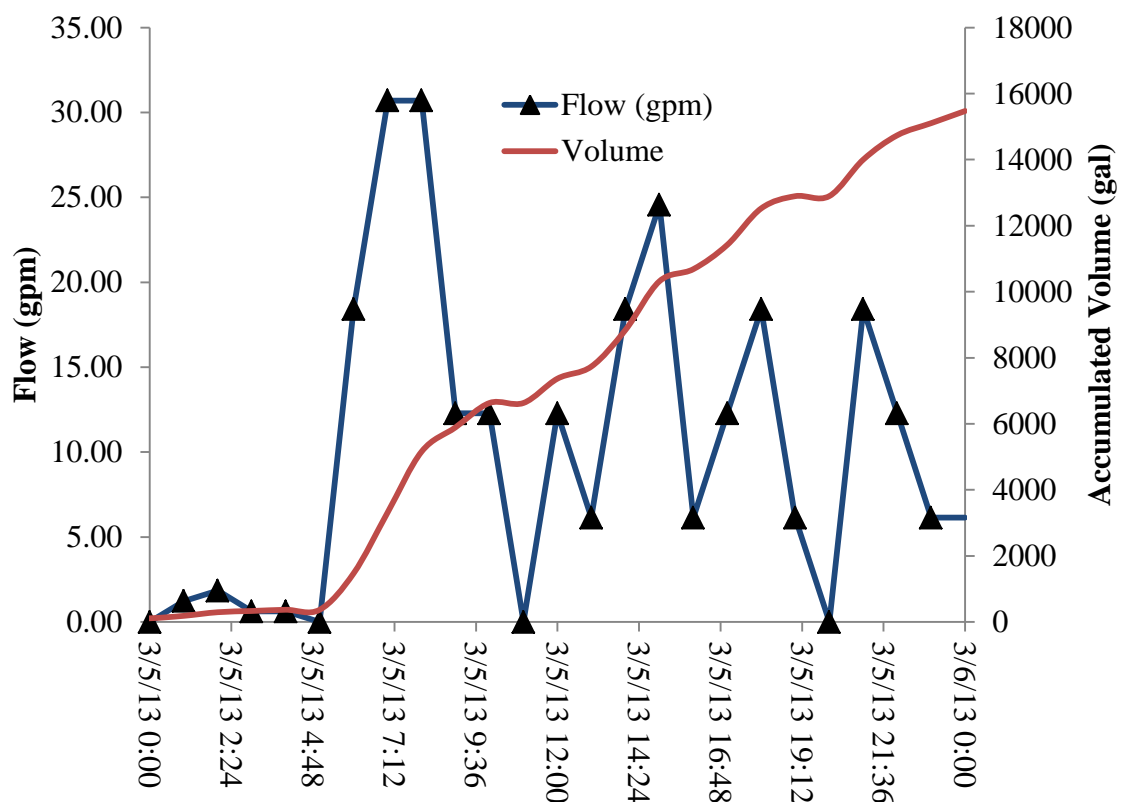


Figure . Estimate of flowrate and accumulated volume for storm event on 3/5/2013

The flow and the sampling events are shown in Figure . The total volume measured by the autosampler was approximately 18,000 gallons. Of the 24 original samples, six representative samples were chosen for detailed analysis (red squares). The samples were analyzed for dissolved and total copper, dissolved organic carbon, total suspended solids, pH, and conductivity. The average pH of the 24 samples was 6.58. The results of the stormwater sample analysis are shown in Figure .

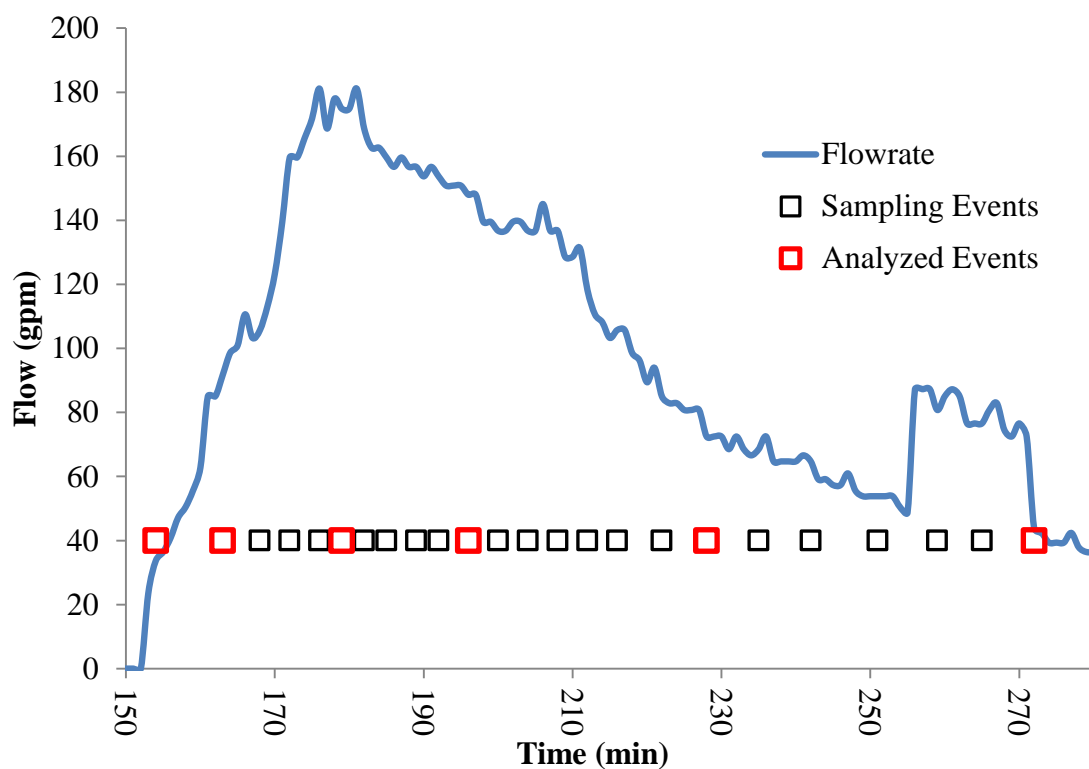


Figure . Flow and sampling events recorded by ISCO 6712 on 3/5/2013

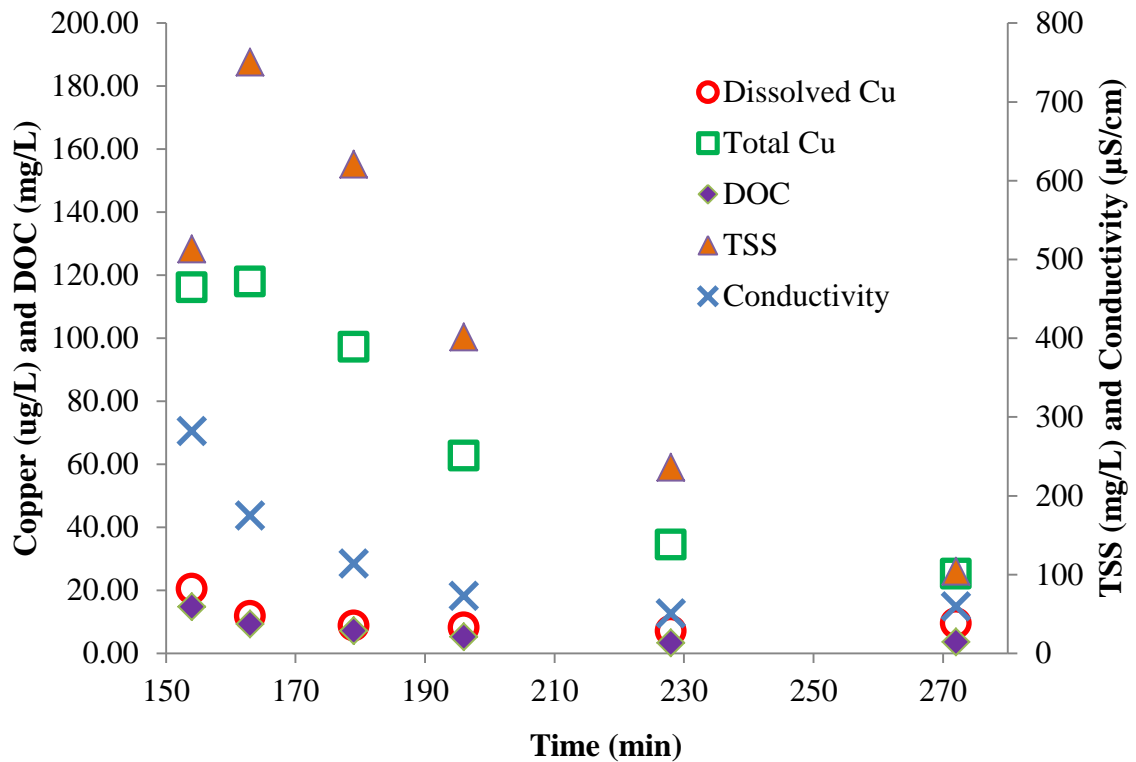


Figure . Water quality data from six analyzed stormwater samples on 3/5/2013

The first flush effect can clearly be seen in the elevated dissolved concentrations in the first sample. The first flush effect can be described most generally as a higher mass of pollutants being washed off at the beginning of a storm than is washed off at the end of a storm. The first portion of the storm flushes most of the pollutants that were deposited on the road surface during the antecedent period before the storm. As the storm progressed, the pollutants deposited on the road are being washed off and, as a result, concentrations decrease over the course of the storm. An increase in measured concentrations was observed in the last sample taken (2nd flow peak), this may have occurred due to small amounts of pollutant accumulating on the road surface between rainfall events in the storm. Similar effects of pollutant concentrations increasing during secondary peak within a storm event has been observed in previous work (Nason et al. 2012). Previous work has shown that dissolved copper is strongly correlated with the concentration of DOC and total copper is correlated with the

concentration of TSS (Nason et al. 2012). The results displayed in Figure are consistent with these correlations. Dissolved copper and DOC reach a maximum at the beginning of the storm and decrease over the duration of the storm event. Conductivity decreases as the storm progresses and is once again evidence of stormwater constituents decreasing in concentration over the course of the storm event. Dissolved copper concentrations measured over the duration of the storm varied between 7-20 $\mu\text{g/L}$. Maximum flow measured at the field-site during the storm event was 180 gpm. Preliminary sampling indicated sufficient flow and dissolved copper at field-site to proceed with design and installation of the filter at the site.

5.4 Site Survey and Permitting

A survey was performed to assess relative distances and elevation of the sites features. A Leica model Viva TS11 total station was used to perform the land survey. The northing, easting, and elevation data was recorded on paper and then later entered into AutoCAD Civil 3D via a text file. A basic overview of the existing ground at the site is shown in Figure .

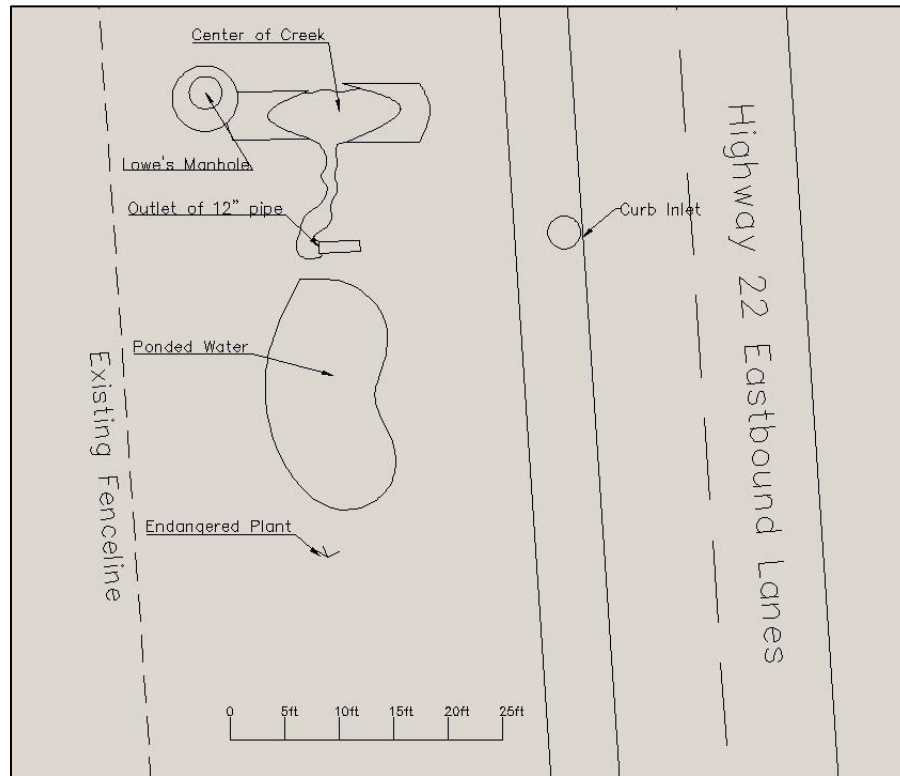


Figure 1. Overview of field site

A permit was acquired to break ground and perform experiments on ODOT right of way. The layout of site features was proposed in the permitting process. This information was used to check for possible safety problems or inconveniences to ODOT maintenance personnel. During the permitting process, attention was brought to a protected plant and ponded water near the site. However, the survey revealed that the plant was well away (>30ft) from any place of disturbance (Figure 1). Ponding occurred because the existing ground at the site did not allow proper drainage from the 12" pipe to the creek bed. Before installing the filter bed, a channel was excavated to improve drainage of the 12" pipe. After channel improvements, it was observed that water stopped ponding and it was decided that more drainage was not necessary. Elevations measured during the survey revealed there is no slope between the outlet of the 12" pipe and manhole (Figure 2). As such, the only available hydraulic head to facilitate flow through the filter is between the outlet of the 12" pipe and the existing

creek bed. The elevation difference between the invert of the 12” pipe and the creek bed is 1ft.

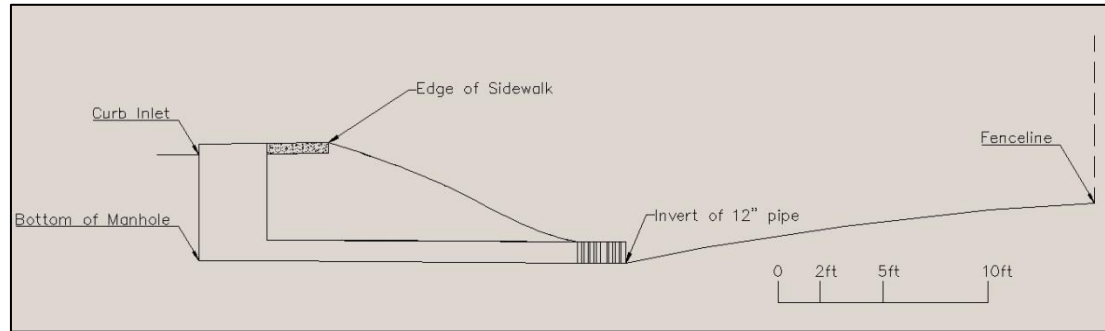


Figure . Cross section of site along existing 12” HDPE pipe

5.5 Filter bed layout

While searching for a means to separate a smaller design flowrate from the total stormwater flow, exploratory hydraulic conductivity tests were performed with an 8” diameter polycarbonate column. The aim of the tests was to assess the hydraulic conductivity of filter materials including Apatite II™ and pea gravel. After performing the tests it was determined that Apatite II™ and or pea gravel provide little resistance to flow. As a result, an additional layer of sand was added. Results from these experiments are displayed in the Appendix. Sand was excluded from the final filter configuration due to the possibility of sand contributing to the removal of copper and poor control of the flowrate delivered to the filter. The final filter configuration is shown in Figure . The bottom of the filter was designed to be drained by a 2” PVC under drain assembly. The under drain was covered with 3” of pea gravel. A 4” layer of fishbone media was placed above the pea gravel. A final 1” layer of pea gravel was added on top of the fishbone to prevent floatation. ODOT drainage unwoven geotextile type 1 (85gpm/ft² hydraulic capacity) was purchased from ACF West Inc. A 4’ x 4’ piece of geotextile was placed between each layer in the filter bed to keep layers separated.

Freeboard
Pea Gravel (1")
Geotextile
Apatite II™ (4")
Geotextile
Pea Gravel (3")

Figure . Layout of filter bed configuration

The headloss through the filter bed was estimated by the Ergun equation (Eq. 5-3), which is typically used to calculate pressure drop across packed bed filters and has been used in the design of rapid sand filters (McCabe 2005).

$$H_L = \left[\frac{150v\mu(1-\varepsilon)^2}{D_p^2\varepsilon^3} + \frac{1.75v^2\rho(1-\varepsilon)}{D_p\varepsilon^3} \right] * \frac{L}{\rho g} \quad (\text{Eq. 5-3})$$

H_L is the headloss (m), v is the velocity (m/s), ε is the porosity (unitless), D_p is the average particle diameter (m), μ is the kinematic viscosity (N-s/m²), ρ is the density of water (1000 kg/m³), L is the bed depth (m), and g is gravity (9.81 m/s²). The headloss was then converted to units of feet.

After calculating a modified Reynolds number and friction factor, the headloss across the filter was calculated. The calculated headloss through the bed is predicted to be negligible with the designed bed configuration (Table).

Table . Summary of headloss calculations

Q (gpm)	Superficial Velocity (gpm/ft ²)	Re	H _L (ft)	Z ₁ -Z ₂ (ft)
0	0	0	0	0
2	0.13	1.92	1.31E-07	1.32E-07
4	0.25	3.84	2.88E-07	2.93E-07
6	0.38	5.75	4.72E-07	4.83E-07
8	0.5	7.67	6.82E-07	7.01E-07
10	0.63	9.59	9.18E-07	9.48E-07
12	0.75	11.51	1.18E-06	1.22E-06
14	0.88	13.43	1.47E-06	1.53E-06
16	1	15.34	1.78E-06	1.86E-06
18	1.13	17.26	2.13E-06	2.22E-06
20	1.25	19.18	2.49E-06	2.62E-06
22	1.38	21.10	2.89E-06	3.03E-06
24	1.5	23.02	3.31E-06	3.48E-06

The Bernoulli equation with headloss was derived for system conditions.

$$\frac{P_1}{\gamma} + \frac{v_1^2}{2g} + z_1 = \frac{P_2}{\gamma} + \frac{v_2^2}{2g} + z_2 + H_L$$

$$0 + 0 + z_1 = 0 + \frac{v_2^2}{2g} + z_2 + H_L$$

$$z_1 - z_2 = \frac{v_2^2}{2g} + H_L \quad (\text{Eq. 5-4})$$

The required elevation difference (Eq. 5-4) between the inlet and outlet was calculated for each flow and headloss. The results are summarized in the last column of Table . In summary, very little head is required to pass these low flowrates. As a result, there will be no accumulated head over the filter without some additional constriction or structure downstream of the filter.

5.6 Inlet Structure

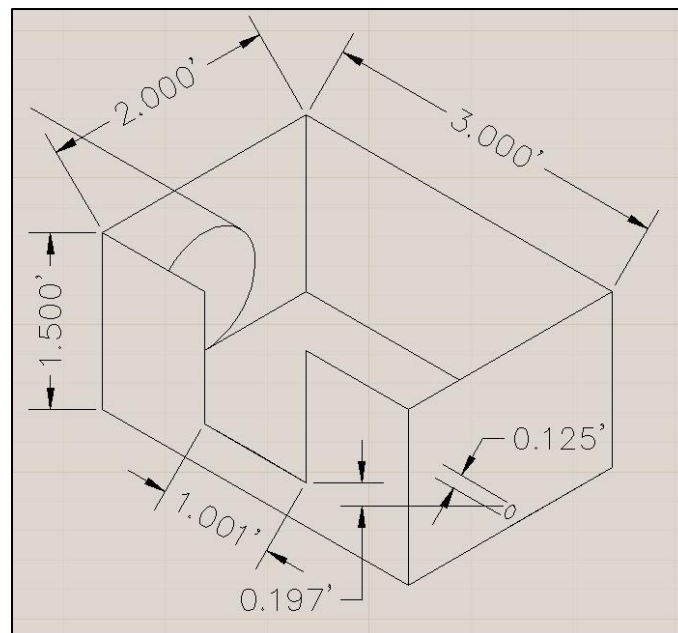
With minimal headloss to control the flow through the system, design of an external hydraulic control structure was necessary. The goal of designing the inlet structure was to create both a sampling location and a mechanism to control the flow to the filter. Given that the influent flowrate is dynamic, the system was designed such that a reasonably constant testable flowrate could be delivered to the filter bed. The method of flow control chosen for this work uses a submerged circular orifice delivering flow to the filter and a side weir to maintain approximately constant head over the orifice at the design flowrate of 16 gpm. Using the Bernoulli equation with exit losses (Eq. 5-5), the head above the orifice as a function of orifice diameter and flowrate (velocity) was solved.

$$z_1 - z_2 = \frac{V_2^2}{2g} + K \frac{V_2^2}{2g} \quad (\text{Eq. 5-5})$$

Orifice diameter was optimized through the variation of flowrate and orifice sizes. An orifice diameter of 1.5” was chosen. With an orifice diameter of 1.5” and a flowrate of 16 gpm, the required head is 2.36” above the top of the orifice (Figure). The exit loss coefficient (K), is 0.5 for square edged exits (Mays 2005). At flowrates less than 16 gpm, all of the flow will be delivered to the filter. At flowrates above 16 gpm, water will begin to spill over the weir. The effect of flow increasing above the design flowrate of 16 gpm is shown in Table . If actual field results differ, the orifice can be replaced by another size and/or the overflow weir height can be altered.

Table . Comparison of total system flow and flow through the bed

Head over weir (in)	Head over orifice (in)	Total Flow (gpm)	Flow to Filter (gpm)
0	2.36	16.00	16.00
0.5	2.86	28.61	17.61
1	3.36	51.36	19.09
1.5	3.86	80.42	20.46
2	4.36	114.33	21.75
2.5	4.86	152.24	22.96
3	5.36	193.53	24.12
3.5	5.86	237.75	25.22

**Figure . Schematic of inlet structure (dimensions are in feet)**

The inlet box was constructed with 3/8" polycarbonate sheeting. The outlet of the box was fitted with a threaded 1-1/2" bulk head tank fitting to deliver water to the filter bed. The weir structure shown on the side of the box was cut to height and tested hydraulically. A scrap piece of 12" HDPE culvert was acquired from ODOT's maintenance facility and used to accurately cut the box to fit around the ribbing of the

culvert. Before field installation, the inlet box was hydraulically tested. The hydraulic test was performed in the laboratory with a bucket, stopwatch, and scale. The inlet box was filled with a hose and flow was allowed to reach steady state before measurements were taken. After varying the overflow weir height, the optimal height was found to be 3.5" above the bottom of the inlet box and resulted in a measured flowrate of 14.6 gpm. During a given storm event, the total flowrate will likely reach values higher than 16 gpm, resulting in slight increases in flow delivered to the filter (Table). The decision was made to use the 3.5" overflow weir height and have a smaller (14.6 gpm) minimum flowrate to the filter. The weir height can be adjusted if necessary after deployment in the field and evaluation during actual storm conditions.

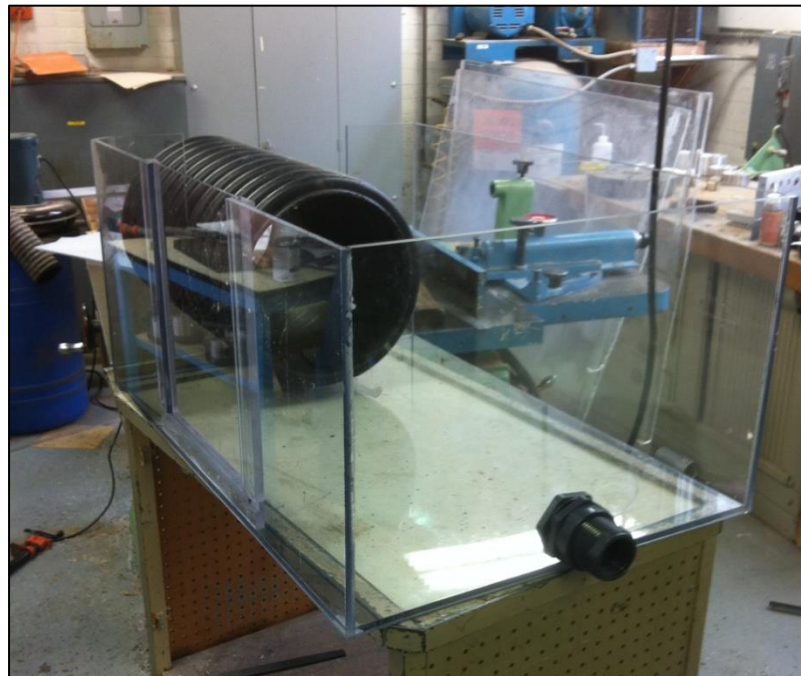


Figure . Constructed inlet box

5.6 Outlet Structure

The outlet weir box was designed to serve as a sampling location and to house a weir structure to measure the flow through the filter bed. The box was designed to be connected in-line with the 2" under drain from the filter bed. The weir structure in the

outlet box was designed to allow measurement of the flowrate through the bed. A 1/8" diameter stainless steel bubble tube was included in the design to be used in conjunction with the bubbler flow module on the ISCO 6712 autosampler. Along with these features, a diffuser plate was designed to reduce the turbulence of the water exiting the filter bed and entering the outlet box.

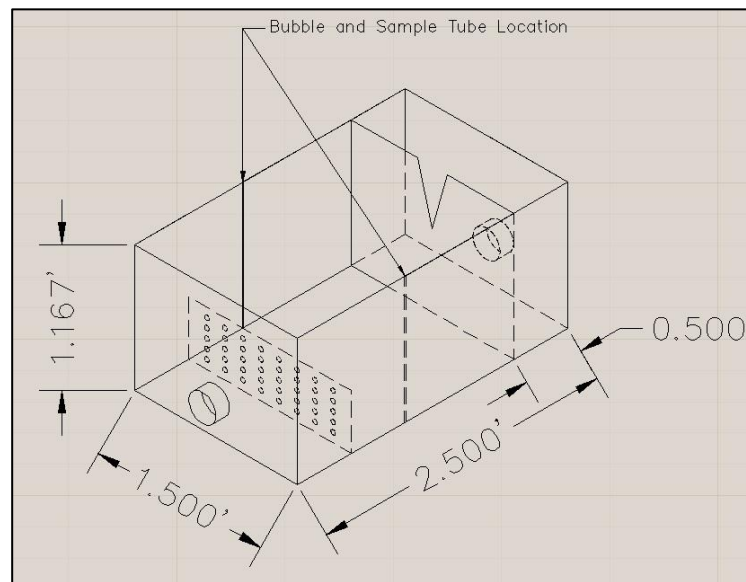


Figure . Schematic of outlet box (dimensions are in feet)

Using the ISCO open channel flow manual as a guide (Walkowiak 2008), the weir structure in the outlet box was designed to accurately measure the expected flowrates through the filter. To avoid sensing drawdown effects at the weir, the bubble tube location was positioned behind the weir a distance two times the height of the weir (1'). The crest of the v-notch was beveled (45°) to reduce the water contacting the downstream side of the weir and promoting ventilation of the nappe. The v-notch weir equation was used to calculate head and flowrate relationships (Figure).

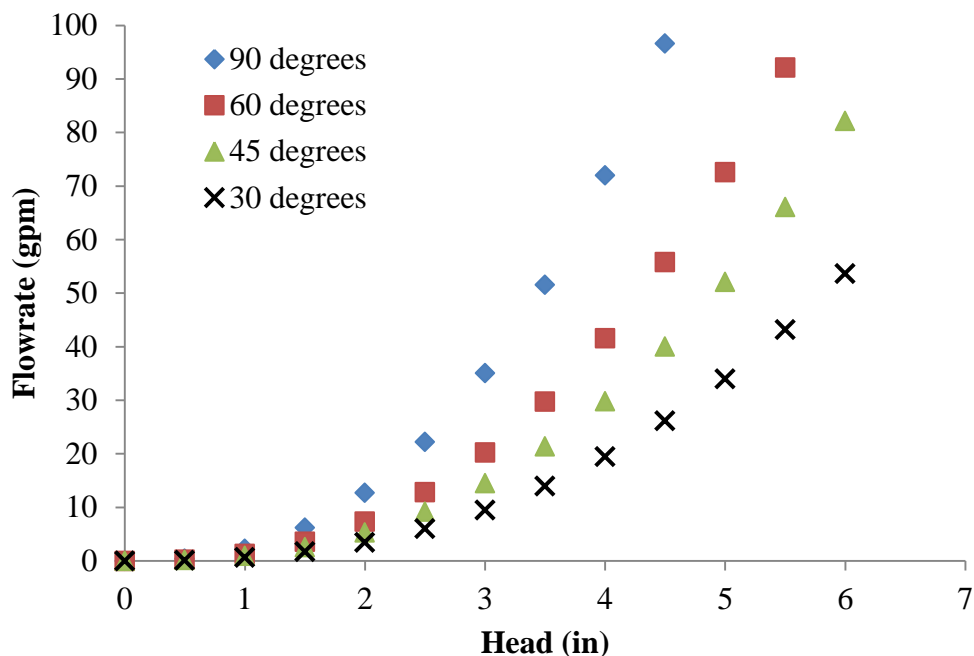


Figure . Comparison of v-notch weir angles

Comparing the different v-notch angle options for the outlet weir structure, a v-notch angle of 30° was chosen because of the higher sensitivity at the design flowrate of 16 gpm. The 30° v-notch weir has the lowest slope around 16 gpm, but it also has adequate capacity to measure flowrates up to about 50 gpm. This was considered in the event that future work examines the effect of varying hydraulic loading rates (increasing the flow through the filter bed).

The outlet box was constructed with $3/8''$ polycarbonate sheeting (Figure). The outlet of the box was fitted with two threaded $2''$ bulk head tank fitting to deliver water from the filter bed to the outlet box and then discharge to the creek. The 30° v-notch weir structure was tested hydraulically to verify the v-notch weir model equation. The hydraulic test was performed in the laboratory with a bucket, stopwatch, tape measure and scale. The outlet box was filled with a hose and flowrate was allowed to reach steady state before measurements were taken. A depth of $3.5''$ above the crest of the v-notch was measured with a tape measure. Figure , estimates a flowrate of 14 gpm with a 30° v-notch angle. The measured flowrate with a bucket, stopwatch, and scale was

14.2 gpm. This results in a percent difference of 1.43% from the predicted value (14 gpm), which is well within the approximate 5% error associated with v-notch weirs (Walkowiak 2008).



Figure . Constructed outlet box

5.7 Filter bed construction

The filter bed was constructed with 2 x 4 lumber and $\frac{1}{2}$ " plywood. The filter dimensions (4' x 4' x 1') were determined from the design flowrate and filter bed layout. The filter bed layout includes 8" of total media and was designed to have 4" of freeboard. The first constructed piece was the frame and floor of the filter bed shown in Figure .



Figure . Filter bed frame and floor

A second frame was constructed to structurally support the top of the filter bed. The top and bottom frames were connected with small vertical pieces of 2 x 4. Once the frame was constructed, the inside was lined with $\frac{1}{2}$ " plywood. The only limiting factor when constructing with plywood was that the sheet was only 4' wide. This resulted in losing 1" in each dimension, the resulting inside dimensions of the filter bed were 3'11" x 3'11". The final constructed filter bed is shown in Figure .



Figure . Constructed filter bed

The under drain for the system was built with 2" PVC pipe and drilled with a 3/8" holes. The holes were distributed evenly and spaced 2" apart. The drainage system was threaded into a 2" bulkhead fitting to connect to the outlet box. The delivery system to the top of the filter bed was built with 1-1/2" PVC pipe and meant to distribute the influent to the filter bed (Figure). The system will deliver water to three 6" diameter channels that will be resting on top of the filter bed material.

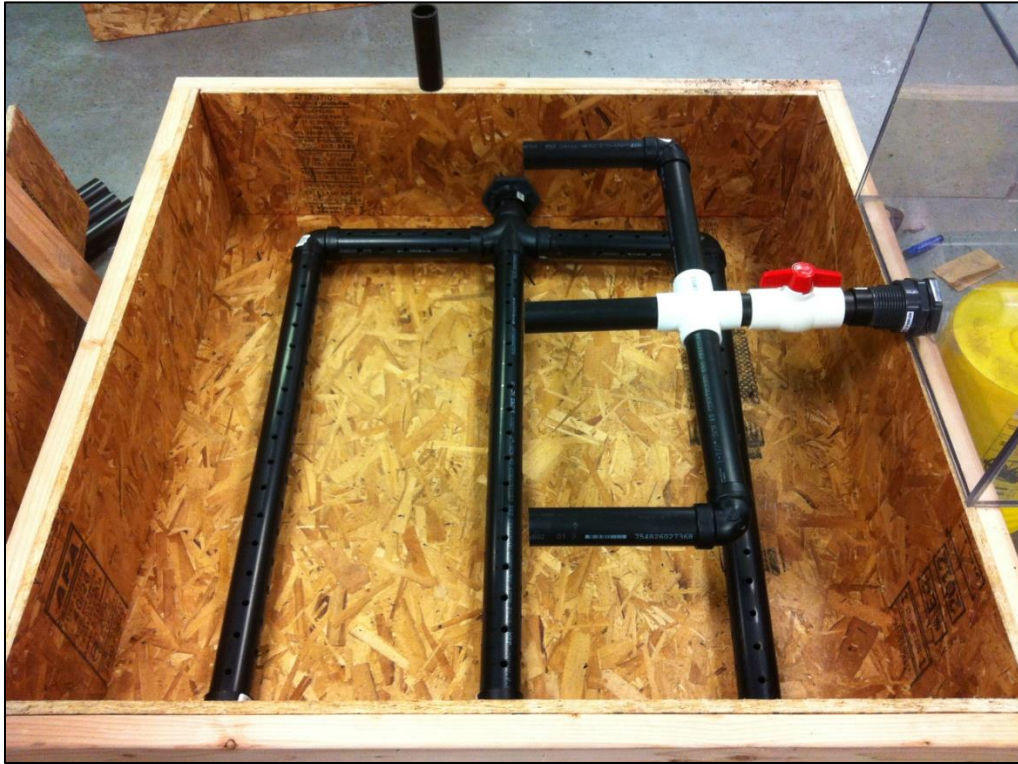


Figure . 2" PVC under drain and 1 ½" PVC delivery system

A lid for the filter bed was constructed with 2 x 6 lumber and ½" plywood shown in Figure . A notch in the lid was cut to accommodate the 1-½" pipe that delivers water to the filter bed.



Figure . Constructed filter lid

5.8 Installation of filter

The installation of the filter was performed over the course of three days. It took a day each to install the inlet structure, filter bed, and outlet structure, respectively. Prior to installing the filter, a 20' x 20' fence was installed at the site to increase security. The fence was installed by Oasis fencing (Figure). Excavation was made difficult by existing rocks and roots in the subsurface.



Figure . Installed security fence

The first piece installed was the inlet structure. A hole 2' x 3' wide and 3' deep was excavated by hand with shovels to accommodate the inlet structure. The inlet structure was slipped onto the ribbing of the 12" HDPE culvert and then held in place while backfilling dirt. The inlet structure was then leveled and silicone was used to seal the inlet structure to the pipe.



Figure . Installed inlet structure

The filter bed was lined with 6 mil polyethylene sheeting prior to installation. A 4' x 4' wide and 1-½' deep hole was excavated by hand to position the filter bed below the inlet structure. The filter bed was then leveled and checked for proper elevation (Figure).



Figure . Installed filter bed with polyethylene sheeting

The last piece installed was the outlet structure. A hole 3' x 2' wide and 1.5' deep was excavated by hand to install the outlet structure. As shown in Figure , the outlet was connected to the filter bed with 1-½" flexible tubing. The system was designed to allow some flexibility in the elevation of the outlet structure. A channel was dug from the outlet structure to existing creek bed to allow for drainage of the system.



Figure . Installed outlet structure

Before the placing of the Apatite II™ layer in the filter bed, a 4' x 4' piece of unwoven geotextile material was installed (Figure). As shown in Figure , a 4" layer of Apatite II™ media was installed on top of the geotextile fabric and leveled to provide a uniform layer thickness. Another 4' x 4' piece of geotextile fabric was used to cover the Apatite II™ layer. The final layer of gravel was installed to help distribute the flow and impede the floatation of the Apatite II™ layer (Figure).



Figure . Geotextile material installed between gravel and Apatite II™ layers



Figure . Installed 4" layer of Apatite II™ media



Figure . Final gravel layer installed in filter bed

6 Conclusions

Single-element removal capacity relationships were developed to characterize the removal of copper and zinc by Apatite II™. Drawing on the results from the batch testing and parameters previously estimated for a full-scale Apatite II™ installation (Huang 2012), rapid small scale column tests (RSSCT) were utilized to assess the effects of varied influent concentration on copper removal with Apatite II™. Prospective field sites were visited and a decision matrix was constructed to select the best possible site for field-scale testing. Storm events were sampled from one site in Salem, OR, to confirm sufficient concentrations of copper and flow for assessing future field-scale copper removal with Apatite II™. First flush and flow-paced samples were collected to characterize the stormwater quality parameters to inform the filter design process. A land survey was performed to assess existing site characteristics; these site characteristics were used to perform the design of a field-scale stormwater filter. As a final result, the designed stormwater filter system was constructed and then installed at the selected field site. Specific conclusions and practical implications from laboratory and field studies are discussed as follows.

6.1 Results from laboratory experiments

The major findings of the laboratory results from the present work are summarized as follows.

1. Copper and zinc were effectively removed from synthetic stormwater runoff by Apatite II™.
2. Zinc removal by Apatite II™ was well characterized by a Langmuir isotherm. Copper removal by Apatite II™, was well described by a linear isotherm.
3. Column studies showed that copper breakthrough was independent of influent concentration. The extent of copper removal with Apatite II™ appears to be controlled by the solubility of copper containing precipitates and is a strong function of pH.

4. The addition of NOM inhibits the removal of copper with Apatite II™.
5. Initial studies showed compost can effectively remove copper to approximately 50 µg/L.

6.1.1 Practical Implications from laboratory experiments

In terms of full-scale application, the release of previously deposited metals that was seen in the column experiments is a major drawback. When designing field-scale systems, replacement of Apatite II™ media before this occurs is necessary. The ability of phosphate from Apatite II™ to buffer pH in continuous flow systems decreases over long operation times. The fact that copper breakthrough with Apatite II™ is independent of influent concentration is useful for stormwater treatment due to the variability of copper concentrations found in stormwater. Apatite II™ effectively removes copper and zinc at trace levels, but was found to release large amounts of phosphate (~20 mg/L). The United States Environmental Protection Agency (USEPA) recommends that phosphate levels be kept below 0.1 mg/L to avoid accelerated eutrophication (Tillers 2003). Phosphate release from Apatite II™ is of concern because phosphate is a nutrient for algae and can cause eutrophication when discharged to aquatic systems. It is unclear exactly how the release of phosphate would change at full scale. It is likely that initial phosphate release will result in concentrations as high as 10-20 mg/L, but would decrease to less than 5 mg/L with time. It appears that this release would continue for the duration of operation. Consequently, the impact on receiving waters would be dictated by the volume of water treated at each site. It is possible that a media designed to sequester phosphate could be amended to mediate this release. However, the presence of phosphate is a key factor in the removal of both copper and zinc, a fact that must be considered in design of metal remediation systems with Apatite II™.

6.2 Results from field experiments

The major findings of the field experiments from the present work are summarized as follows.

1. Site along Highway 22 in Salem, OR has desirable characteristics to assess the removal of copper with Apatite II™ at field-scale.
2. Preliminary sampling indicates sufficient flow and dissolved copper at field-site. High levels of total suspended solids (500 mg/L) and dissolved organic carbon (20 mg/L) were detected.
3. Full size Apatite II™ was found to provide little to no resistance to flow at the design flowrate.

6.2.1 Practical Implications from field experiments

At extended filter operating times, high concentration of TSS (100-750 mg/L) measured in initial stormwater sampling could induce filter bed clogging.

Consequently, settleable suspended solids may deposit in the inlet structure prior to stormwater being delivered to the filter bed. Before each sampling event it is recommended that any debris and or standing water should be removed to ensure representative sampling. If the TSS loading problem persists, cleaning of the manhole catch basins is recommended. High concentrations of NOM were measured in initial stormwater sampling. Subsequent batch studies should be designed to test relevant NOM concentrations with respect to concentrations measured at the field site (≤ 20 mg/L). Seasonal changes in the groundwater table at the field site may require readjustment of the outlet weir box's elevation to maintain proper filter operation. As discussed previously, large amounts of phosphate may be released in the effluent of the field-scale filter bed. Filter bed arrangement could be altered to include a media to remove the released phosphate. As stated previously, the presence of phosphate is an integral part of metals removal and a necessary consideration when designing a system to remove metals and phosphate. The layer of Apatite II™ media could be swapped out to

experiment with alternative media such as compost. Apatite II™ will most likely release odor after extended filter operation. This effect may be minimized by ensuring the filter bed lid is properly installed during filter operation.

Removal of dissolved copper from highway stormwater is important because of the demonstrated negative effects on juvenile salmon (Sandahl et al. 2007). Extensive effort has been made in the Pacific Northwest to restore preexisting salmon habitat (removal of fish blockages). To improve utilization of salmon habitat expansion, removal of olfactory inhibitors such as dissolved copper is important. This study has shown Apatite II™ has an exceptional removal capacity for copper and zinc in stormwater runoff, resulting in effluent copper concentrations below levels that adversely affect juvenile salmon (<2 µg/L). A platform (field-scale filter) was designed and constructed to allow future testing of copper removal with Apatite II™ in actual highway stormwater. Future testing of Apatite II™ at field-scale is important to understand how constituents (NOM) of actual stormwater will affect removal capacity of dissolved copper. Apatite II™ represents a promising alternative media to remove dissolved copper highway stormwater runoff.

6.3 Future work

Potential future works to add to the understanding of metals removal with Apatite II™ in both the laboratory and field setting are outlined here. Batch and column experiments with the addition of natural organic matter in synthetic stormwater runoff could be conducted to investigate the extent to which organic matter influences the removal of copper and zinc. Sampling of the influent and effluent of the field-scale filter during an actual storm event could be performed to characterize the removal of copper with Apatite II™ at field-scale. Operational parameters of the field-scale filter such as flowrate and outlet box elevation could be varied to experiment with the effect of hydraulic loading rates and submerged media depth on copper removal. Apatite II™

media could be replaced with alternative media such as compost to compare copper removal with different filter bed media.

Appendix

Hydraulic Conductivity Experiments

Permeability (hydraulic conductivity) tests were performed to assess the hydraulic conductivity of filter materials including Apatite II™ and pea gravel. After performing initial tests it was determined that Apatite II™ and or pea gravel provide little resistance to flow. As a result, an additional layer of sand was added. The standard test method for permeability of granular soils (ASTM-D 2434) was used. These tests were conducted with an 8” diameter polycarbonate column. The layout of filter bed materials tested is shown in Figure . The sand layer thickness was varied to assess its ability to restrict the flow and control the flowrate to the filter bed.

Pea Gravel (1")
Play Sand (2",3",4")
Fish Bone (4")
Pea Gravel (4")

Figure . Layout and thickness of material layers

The outlet of the column was raised to the elevation of the top layer of gravel. As a result, the measured head of water above the top gravel layer corresponds to the hydraulic gradient in the system (ΔH). For each measurement, the head was allowed to reach steady state (constant head). Water was delivered with a peristaltic pump delivering flowrates between 0-2000 mL/min. All layers were wet packed, to reduce air bubbles formation in the media. Equation A-1 was used to calculate the hydraulic conductivity of the filter bed. Flowrate divided by cross-sectional area was plotted on the ordinate and hydraulic gradient divided by the depth of the filter bed was plotted

on the abscissa. The resulting hydraulic conductivities (slope) were calculated based on a best-fit line (Figure).

$$\frac{Q}{A} = K_H \frac{\Delta H}{L} \quad (\text{Eq. A-1})$$

Where Q is flowrate (ft^3/day), A is the cross-sectional area (ft^2), K_H is the hydraulic conductivity (ft^3/day), ΔH is the change in head (ft), and L is the bed depth (ft).

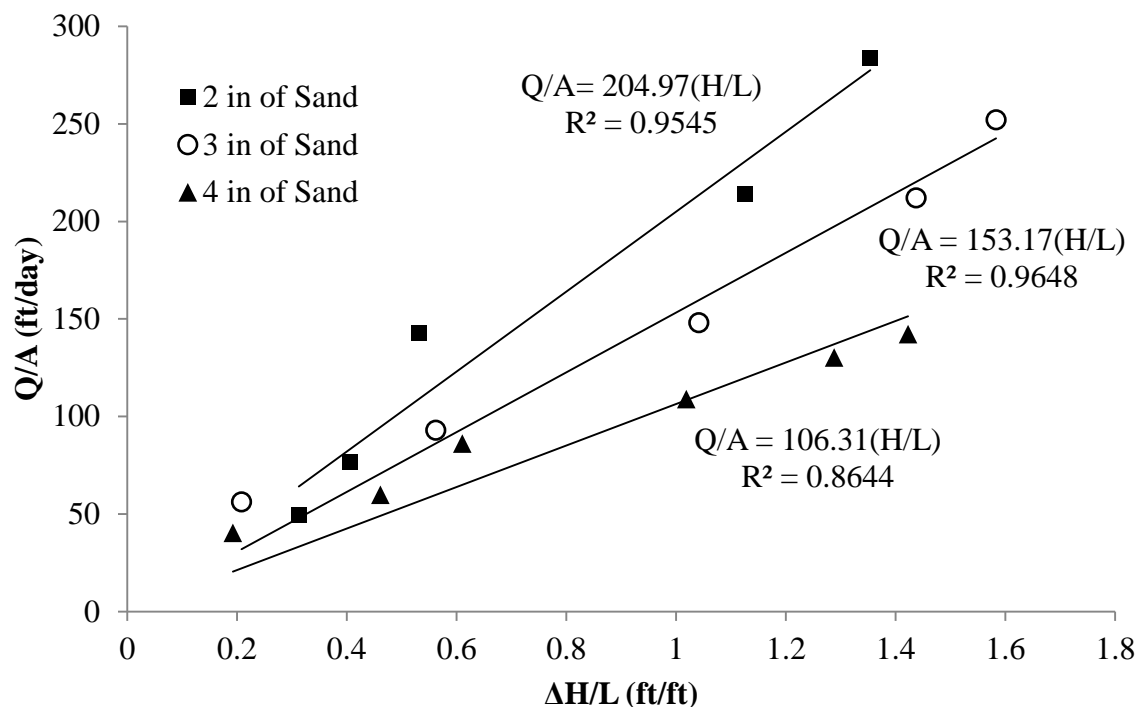


Figure . Hydraulic conductivity values (slope) fitted from experimental data

A range of flowrates were tested on three experimental setups. Three sand layer thicknesses were tested (2", 3", 4"). The resulting hydraulic conductivities were 204.97 ft/day, 153.17 ft/day, and 106.31 ft/day, respectively. The estimated hydraulic conductivity was found to decrease as sand layer thickness increased. This is to be expected considering the sand has the most resistance to flow. After consideration of available head at the field site and poor hydraulic control provided by the sand layer, the sand layer was excluded from the final filter bed layout.

Compost Batch Equilibrium Experiment

Solutions containing 1000 $\mu\text{g/L}$ copper, 0.185 M NaHCO_3 , and 0.100 M NaCl , and a blank solution containing only NaHCO_3 and NaCl , were made and the pH of each solution was adjusted to approximately 6. Samples of compost (0.500 g, 1.00 g, and 3.00 g) were measured out and added to 100 mL of the copper solution. 1.00 g of compost was added to 100 mL of the blank solutions. All sample concentrations were tested in triplicate. The samples were then placed in a tumbler for 48 hours. Then, the samples were filtered through a 0.45 μm filter and placed in sample tubes to be analyzed with the ICP-AES. Compost used in the batch studies was sieved and retained on the #10 mesh. Effluent concentrations of ions in solution were analyzed by the ICP-OES and ion chromatography.

The whole compost showed removal efficiencies of about 93-95% while the sieved compost showed removal efficiencies of around 94%, as seen in Table 8. The larger variation in results from the whole compost is likely due to larger debris in the compost, twigs, dirt, etc., which have a smaller surface area to volume ratio and would greatly affect copper removal at small compost doses (Seelsaen et al. 2007). The samples of whole compost were analyzed using the ICP-AES which has a detection limit of around 100 ppb copper, which could also affect results. The results from the sieved compost show that masses between 0.500 and 3.00 grams of compost do not largely affect removal efficiencies. At compost doses tested, equilibrium concentrations of dissolved copper correspond well with values for concentrations of copper found to leach from compost (50.7 mg/kg Cu^{+2}) (Seelsaen et al. 2007). This suggests compost has the ability to effectively remove dissolved copper from solution, but only to concentrations (60 $\mu\text{g/L}$) typically found in source materials used to generate compost.

Table . Average equilibrium concentrations of dissolved copper in batch studies

Compost Dose (g)	Sieved ($\mu\text{g/L}$)	Whole ($\mu\text{g/L}$)
Blank	10.8	22.0
0.500	58.0	64.7
1.00	58.6	55.4
3.00	58.4	56.3

Table . Average anion concentrations (mg/L) at equilibrium in batch studies

Compost Dose (g)	Cl^-	SO_4^{2-}	PO_4^{3-}	NO_3^-
Blank	43.7	7.50	5.57	>0
0.500	41.5	4.22	3.73	>0
1.00	39.3	7.66	5.15	>0
3.00	19.8	7.43	5.46	>0

Chloride, Sulfate, Phosphate, and Nitrate were present in detectable amounts in the solution after tumbling for 48 hours (Table). Chloride was present in high concentrations, but this was expected since the compost contains food waste (Seelsaen et al. 2006). Nitrate was detected by the ion chromatography, but the standards were much higher than the concentrations present in solution making it difficult to quantify the actual concentrations. Further investigation of compost is necessary to characterize copper removal mechanisms and feasibility of full-scale implementation.

Calculation of bed life for hypothetical full-scale system

Assumptions:

Average annual rainfall = 39 inches

Width of packed bed = 6 ft

Depth of packed bed = 4 in.

Width of roadway = 60 ft

Influent copper concentration = 100 µg/L

Acceptable effluent concentration = 1 µg/L ($C_{out}/C_{in} = 0.01$)

Calculations:

Time to breakthrough ($C_{out}/C_{in} = 0.01$) in the small column = 50 hr (2.08 d)

(from shortest breakthrough between the two tests shown in Figure)

Time to breakthrough ($C_{out}/C_{in} = 0.01$) at full scale (continuous flow)

$$t_{LC} = t_{SC} \left(\frac{R_{LC}}{R_{SC}} \right)^2 = 2.08 \text{ d} \left(\frac{0.84\text{mm}}{0.3585\text{mm}} \right)^2 = 11.42 \text{ d}$$

Specific volume treated at breakthrough ($C_{out}/C_{in} = 0.01$) at full scale

$$\frac{V_b}{A} = v_{LC} t_{LC} = 58.67 \frac{\text{m}^3}{\text{m}^2 \cdot \text{d}} \cdot 11.42 \text{ d} = 670 \frac{\text{m}^3}{\text{m}^2}$$

Specific volume of stormwater needing treatment at the 185th and Cornell Road site

$$\frac{\text{volume of rainfall}}{\text{surface area of media}} = \frac{\left(39.05 \frac{\text{in}}{\text{yr}} \right) \left(\frac{1 \text{ ft}}{12 \text{ in}} \right) (60 \text{ ft})(\text{length ft})}{(6 \text{ ft})(\text{length ft})} = 32.5 \frac{\text{ft}^3}{\text{ft}^2 \cdot \text{yr}} = 9.92 \frac{\text{m}^3}{\text{m}^2 \cdot \text{yr}}$$

Bed life

$$t_{life} = \frac{\text{specific volume treated at capacity}}{\text{specific volume of runoff per year}} = \frac{670 \frac{\text{m}^3}{\text{m}^2}}{9.92 \frac{\text{m}^3}{\text{m}^2 \cdot \text{yr}}} = 67.5 \text{ yr}$$

References

- APHA, AWWA & WEF. 2005. *Standard Methods for the Examination of Water and Wastewater*. Washington, DC: APHA, AWWA, WEF.
- Benjamin, M. M. 2010. *Water chemistry*. Boston: McGraw-Hill.
- Champagne, P. & C. Li (2009) Use of Sphagnum peat moss and crushed mollusk shells in fixed-bed columns for the treatment of synthetic landfill leachate. *Journal of Material Cycles and Waste Management*, 11, 339-347.
- Clark, S. & R. Pitt. 1999. Stormwater Treatment At Critical Areas - Evaluation of Filtration Media. ed. E. P. Agency. Cincinnati.
- Conca, J. L. & J. Wright (2006) An apatite II permeable reactive barrier to remediate groundwater containing Zn, Pb and Cd (vol 21, pg 1288, 2006). *Applied Geochemistry*, 21, 2187-2200.
- Crittenden, J. C., J. K. Berrigan & D. W. Hand (1986) Design of rapid small-scale adsorption tests for a constant diffusivity. *Journal Water Pollution Control Federation*, 58, 312-319.
- Davis, A. P., M. Shokouhian & S. B. Ni (2001) Loading estimates of lead, copper, cadmium, and zinc in urban runoff from specific sources. *Chemosphere*, 44, 997-1009.
- Davis, A. P., M. Shokouhian, H. Sharma, C. Minami & D. Winogradoff (2003) Water quality improvement through bioretention: Lead, copper, and zinc removal. *Water Environment Research*, 75, 73-82.
- Grimes, S. M., G. H. Taylor & J. Cooper (1999) The availability and binding of heavy metals in compost derived from household waste. *Journal of Chemical Technology and Biotechnology*, 74, 1125-1130.
- Hewitt, C. N. & M. B. Rashed (1988) Heavy metals in motorway runoff waters. *Heavy metals in the hydrological cycle*, 645-50.
- Hossain, M. A., M. Alam, D. R. Yonge & P. Dutta (2005) Efficiency and flow regime of a highway stormwater detention pond in Washington, USA. *Water Air and Soil Pollution*, 164, 79-89.
- Howell, R. B. 1979. Heavy metals in highway runoff and affects on aquatic biota. In *International conference, management & control of heavy metals in the environment*, 236-8. London.
- Hsieh, C.-h., A. P. Davis & B. A. Needelman (2007) Bioretention column studies of phosphorus removal from urban stormwater runoff. *Water Environment Research*, 79, 177-184.
- Huang, H.-W. 2012. The Assessment of Copper and Zinc Removal from Highway Stormwater Runoff using Apatite IITM. In *Chemical, Biological, and Environmental Engineering*. Corvallis, OR: Oregon State University.
- Johir, M. A. H., J. J. Lee, S. Vigneswaran, J. Kandasamy & K. Shaw (2009) Treatment of Stormwater using Fibre Filter Media. *Water Air and Soil Pollution: Focus*, 9, 439-447.

- Johnson, P. D. 2003. Metals removal technologies for stormwater. In *Industrial Waste Conference*, 739-763. San Antonio: WEF (Water Environment Federation).
- Joshi, U. M. & R. Balasubramanian (2010) Characteristics and environmental mobility of trace elements in urban runoff. *Chemosphere*, 80, 310-318.
- Kayhanian, M. 2010. *Handbook of environmental research / Characteristics of urban highway runoff: general water quality, toxicity and particle size distribution*. Nova Science Publishers, Inc.
- Kim, N. D. & J. E. Fergusson (1994) The concentrations, distribution and sources of cadmium, copper, lead, and zinc in the atmosphere of an urban-environment. *Science of the Total Environment*, 144, 179-189.
- Krejzler, J. & J. Narbutt (2003) Adsorption of strontium, europium and americium(III) ions on a novel adsorbent Apatite II. *Nukleonika*, 48, 171-175.
- Legret, M. & C. Pagotto (1999) Evaluation of pollutant loadings in the runoff waters from a major rural highway. *Science of the Total Environment*, 235, 143-150.
- Li, H. & A. P. Davis (2009) Water Quality Improvement through Reductions of Pollutant Loads Using Bioretention. *Journal of Environmental Engineering-Asce*, 135, 567-576.
- Liu, G. J., X. R. Zhang & J. W. Talley (2007) Effect of copper(II) on natural organic matter removal during drinking water coagulation using aluminum-based coagulants. *Water Environment Research*, 79, 593-599.
- Makepeace, D. K., D. W. Smith & S. J. Stanley (1995) Urban stormwater quality - summary of contaminant data. *Critical Reviews in Environmental Science and Technology*, 25, 93-139.
- Maurer, M. W. 2009. Design and Construction of a Field Test Site to Evaluate the Effectiveness of a Compost Amended Bioswale for Removing Metals from Highway Stormwater Runoff. 72. Washington State Department. of Transportation.
- Mays, L. W. 2005. *Water Resources Engineering*. John Wiley & Sons, Inc.
- McCabe, W. L. 2005. *Unit Operations Of Chemical Engineering*. McGraw-Hill.
- McIntyre, J. K., D. H. Baldwin, J. P. Meador & N. L. Scholz (2008) Chemosensory deprivation in juvenile coho salmon exposed to dissolved copper under varying water chemistry conditions (vol 42, 1352, 2008). *Environmental Science & Technology*, 42, 6774-6775.
- Moran, K. D. 1997. Vehicle brake pads: a significant, but resolvable, storm water runoff problem. In *Water Environment Federation 70th Annual Conference & Exposition*, 493-497.
- Nason, J. A., M. S. Sprick & D. J. Bloomquist (2012) Determination of copper speciation in highway stormwater runoff using competitive ligand exchange - Adsorptive cathodic stripping voltammetry. *Water Research*, 46, 5788-5798.
- ODEQ. 2012. General Permit: National Pollutant Discharge Elimination System-Stormwater Discharge Permit. ed. O. D. o. E. Quality, 93. Portland.
- ODOT. 2012. 2011 Transportation Volume Tables. 91. Oregon Department of Transportation.

- Oliva, J., J. De Pablo, J. L. Cortina, J. Cama & C. Ayora (2010) The use of Apatite II (TM) to remove divalent metal ions zinc(II), lead(II), manganese(II) and iron(II) from water in passive treatment systems: Column experiments. *Journal of Hazardous Materials*, 184, 364-374.
- Oliva, J., J. De Pablo, J. L. Cortina, J. Cama & C. Ayora (2011) Removal of cadmium, copper, nickel, cobalt and mercury from water by Apatite II (TM): Column experiments. *Journal of Hazardous Materials*, 194, 312-323.
- Pitcher, S. K., R. C. T. Slade & N. I. Ward (2004) Heavy metal removal from motorway stormwater using zeolites. *Science of the Total Environment*, 334, 161-166.
- Sabin, L. D., J. H. Lim, K. D. Stolzenbach & K. C. Schiff (2005) Contribution of trace metals from atmospheric deposition to stormwater runoff in a small impervious urban catchment. *Water Research*, 39, 3929-3937.
- Sandahl, J. F., D. H. Baldwin, J. J. Jenkins & N. L. Scholz (2007) A sensory system at the interface between urban stormwater runoff and salmon survival. *Environmental Science & Technology*, 41, 2998-3004.
- Seelsaen, N., R. McLaughlan, S. Moore & R. M. Stuetz (2006) Pollutant removal efficiency of alternative filtration media in stormwater treatment. *Water Science and Technology*, 54, 299-305.
- Seelsaen, N., R. McLaughlan, S. Moore & R. M. Stuetz (2007) Influence of compost characteristics on heavy metal sorption from synthetic stormwater. *Water Science and Technology*, 55, 219-226.
- Sun, X. L. & A. P. Davis (2007) Heavy metal fates in laboratory bioretention systems. *Chemosphere*, 66, 1601-1609.
- Walkowiak, D. K. 2008. *Isco Open Channel Flow Measurement Handbook*. Lincoln, NE.
- Wright, J. & J. Conca (2002) Remediation of groundwater and soil contaminated with metals and radionuclides using Apatite II, a biogenic apatite mineral. *Preprints of Extended Abstracts presented at the ACS National Meeting, American Chemical Society, Division of Environmental Chemistry*, 42, 117-122.
- Wright Water Engineers, I. & I. Geosyntec Consultants. 2011. Pollutant Category Summary: Metals. 64. International Stormwater BMP Database.